

MEASUREMENT OF DIFFUSION COEFFICIENTS
OF
BINARY LIQUID SYSTEMS
BY
THE MOIRE PATTERN METHOD

MEASUREMENT OF DIFFUSION COEFFICIENTS
OF
BINARY LIQUID SYSTEMS
THE MOIRE PATTERN METHOD

by

C.D. Le, B.A.Sc.

A Thesis

Submitted to the Faculty of Graduate Studies
in Partial Fulfilment of the Requirements
for the Degree
Master of Engineering

McMaster University

September 1968

MASTER OF ENGINEERING (1968)
(Chemical Engineering)

McMaster University
Hamilton, Ontario.

TITLE: Measurement of Diffusion Coefficients in Binary Liquid Systems
by the Moiré Pattern Method.

AUTHOR: C.D. Le, B.A.Sc. (Ecole Polytechnique of University of Montreal,
Montreal)

SUPERVISORS: Professors A.E. Hamielec, A.I. Johnson

NUMBER OF PAGES: 91

SCOPE AND CONTENTS:

Experiments were carried out to measure diffusion coefficients of some inorganic and organic binary liquid systems at various concentrations. A diffusion cell of the "shearing type" was used. Photographs of the concentration gradient curves, given by the moiré phenomenon, were taken and analyzed to obtain the concentration profiles. Diffusion coefficients were then calculated according to Fick's second law using a Boltzmann transformation.

Results found were compared with those reported by other investigators. Satisfactory agreement was obtained.

ACKNOWLEDGEMENTS

The author is very grateful for the original ideas and the guidance given to him by Dr. A.E. Hamielec and Dr. A.T. Johnson throughout this project. He also acknowledges with appreciation the help of Dr. W.F. Furter in the modification of the diffusion cell at the Royal Military College.

Sincere thanks is extended to Mr. P. Seto for his most important contribution to the design of the diffusion cell as well as to the realization of this project.

Finally, financial support granted to the author by McMaster University is well appreciated.

TABLE OF CONTENTS

	<u>Page</u>
1. ABSTRACT	1
2. INTRODUCTION	2
3. THEORY	
3.1 Derivation of Fick's Second Law	8
3.2 Relation between the Moiré Pattern and Concentration Gradient Curves	13
4. EXPERIMENTS	
4.1 Apparatus	20
4.1.1 The Diffusion Cell	
4.1.2 Experimental Setup	
4.2 Procedure	22
4.3 Method of Calculation	23
5. RESULTS	26
6. DISCUSSIONS	44
7. CONCLUSIONS AND RECOMMENDATIONS	57
8. NOMENCLATURE	61
9. REFERENCES	63

LIST OF DIAGRAMS

	<u>Page</u>
Figure 1 Deflection of a Light Beam passing through a Medium of continuously varying Refractive Index	15
Figure 2a Disposition of the Diffusion Cell and the Screens	19
Figure 2b Relation between Height of Moiré Curves and Refractive Index Gradient	19
Figure 3a The Diffusion Cell	21
Figure 3b Experimental Setup	21
Figure 4a Procedure	24
Figure 4b Moiré Curve and Concentration Gradient Profile	24
Figure 5a Integration of Moiré Curves	25
Figure 5b Concentration Profile with Corrected x-Origin	25
Figure 6 Dependence of Refractive Index on Concentration - System: Sucrose - Water	27
Figure 7 - ibid - System: Sodium-Chloride-Water	28
Figure 8 - ibid - System: Glycine-Water	29
Figure 9 - ibid - System: Ethyl Acetate-Water	30
Figure 10 - ibid - System: Benzene-Carbon Tetrachloride	31

	<u>Page</u>
Figure 11 Testing of Boltzmann Assumption	
System: Sucrose-Water	33
Figure 12 - ibid -	
System: Sodium Chloride-Water	34
Figure 13 - ibid -	
System: Glycine-Water	35
Figure 14 - ibid -	
System: Ethyl Acetate-Water	36
Figure 15 - ibid -	
System: Benzene-Carbon Tetrachloride	37
Figure 16 Dependence of Diffusion Coefficient on Concentration	
System: Sucrose-Water	39
Figure 17 - ibid -	
System: Sodium Chloride-Water	40
Figure 18 - ibid -	
System: Glycine-Water	41
Figure 19 - ibid -	
System: Ethyl Acetate-Water	42
Figure 20 - ibid -	
System: Benzene-Carbon Tetrachloride	43
Figure 21 Testing of Method of Calculation	
System: Sucrose-Water	50

	<u>Page</u>
Figure 22 Testing of Method of Calculation	
System: Sodium Chloride-Water	51
Figure 23 - ibid -	
System: Glycine-Water	52
Figure 24 - ibid -	
System: Ethyl Acetate-Water	53
Figure 25 - ibid -	
System: Benzene-Carbon Tetrachloride	54
Figure 26 Diffusion Measurement by Laser Interference	60
Table A.1 Estimation of Diffusivities at Infinite Dilution	76
Figure 27 Sample Picture	90
Table A.2 Equations experimentally found for Diffusion Coefficients as Function of Concentration	91

APPENDICES

	<u>Page</u>
Appendix I - Derivation of the Expression for Diffusivities when there is Volume Change on Mixing.	67
Appendix II - Estimation of Diffusivities at Infinite Dilution	75
Appendix III - Computer Programs	80
Appendix IV - Sample Picture; Equations experimentally found for Diffusion Coefficients as Function of Concentration	90

1. ABSTRACT

A diffusion cell of the "shearing type" was used to diminish the effect of convection which is always present when two liquid phases are brought into contact with each other in a diffusion cell. Also a special optical arrangement was used to photograph the refractive index distribution of the system. For those systems with refractive index changing linearly with concentration, the concentration profiles were obtained and diffusion coefficients were calculated at different concentrations.

This optical method gave only fair reproducibility - the deviation among diffusivities found for systems investigated varying from 3 to 10 per cent - however, it permitted rapid analysis and on this basis is recommended for situations where speed is essential and high accuracy is not required.

2. INTRODUCTION

Diffusion has been defined as the process by which material at one part of a system is transported to another part by random molecular motion, due to either thermal agitation or collisional impact.

While self diffusion is a special case where the diffusing particles are identical, rotary diffusion involves a rearrangement of anisotropic particles from a state of preferred order to one of random distribution. The most important mode of diffusion, however, is mutual diffusion where one component of a binary mixture diffuses into the other and vice versa.

The first attempt to describe statistically the relationship between the random molecular motion and diffusion flow was made by Einstein⁽¹⁾ in his discussion of the Brownian motion but fifty years earlier, Fick⁽²⁾ had already established a phenomenological formulation of the diffusion process.

Recognizing that there is an analogy between the transfer of heat by conduction and diffusion of material, Fick adopted the equation for heat conduction, derived by Fourier⁽³⁾ and stated that at constant pressure and temperature, the rate of transfer of material is proportional to the concentration gradient, namely:

$$N = - D \frac{\partial C}{\partial x} \quad (2.1)$$

where N is the rate of material transfer per unit area, $\frac{\partial C}{\partial x}$ is the concentration gradient at a particular time and D , presumed to be a

constant for a given system, is called the "diffusion coefficient" or diffusivity.

In some cases, e.g. diffusion in dilute solutions, D can be considered as a constant while in others, it varies with concentration, particularly for liquid-phase diffusion.

The theoretical and experimental studies in diffusion helped to develop successfully the kinetic theory of gases, the structural discoveries for solids and electrolytes; they are being used in formulating mass transfer processes as well as in the determination of particle size or molecular weight⁽⁴⁾.. Given such a wide application of Fick's first law, extensive research has been carried out to estimate and to measure the diffusion coefficient.

Diffusion in binary gaseous systems has been thoroughly investigated and a number of semi-empirical equations, based on experimental data, have been proposed and tried out successfully at moderate pressures and temperatures. There are equations by Gilliland⁽⁵⁾, Hirschfelder, Bird and Spatz⁽⁶⁾, Slattery and Bird⁽⁷⁾ for diffusivities in binary gaseous system. Some of these equations agree reasonably well with experimental findings. On the other hand, for multicomponent mixtures, the equation of Stefan-Maxwell⁽⁸⁾ is the most widely used.

For measuring gaseous diffusion coefficients, perhaps the most famous method was the one developed by Loschmidt^(9, 10) and later by Stefan^(11, 12, 13) which consisted of a tube divided in two halves by a stopcock. Gases were separately introduced into each half and the diffusion started by opening the stopcock to let the gases contact with each other. Later, Obermayer⁽¹⁴⁾ modified this technique by replacing

the stopcock by two ground discs, rotating upon each other, each connected to one tube. Diffusion coefficients obtained by this method appeared to be very accurate, with a deviation of about 1 percent only.

Diffusion in liquid systems has been given special attention because of the wide need of diffusion coefficients. Many theories have been developed to formulate rigorously the diffusion process in liquids. Among them, the most famous are those by Einstein⁽¹⁾ with a hydrodynamic development for dilute solutions, by Arnold⁽¹⁵⁾ and Eyring⁽¹⁶⁾ who applied the kinetic theory of gases to diffusion of liquids. Later, Crank and Hartley⁽¹⁷⁾ used both thermodynamic and hydrodynamic considerations in their development of a relation between the non-ideality of a system and its diffusion coefficients. Pynn and Fixman⁽¹⁸⁾ extended the hydrodynamic model to concentrated systems while Olander, Gainer and Metzner⁽¹⁸⁾ applied Eyring's theory in the case of dilute solutions of high viscosity. Their technique has been used by Cussler and Lightfoot⁽¹⁸⁾ to obtain an approximation of diffusion coefficients in systems.

For engineering purposes, several correlations have been proposed to estimate diffusion coefficients in dilute solutions. Among them, the Wilke and Chang⁽¹⁹⁾ correlation was obtained from data for 285 points among 251 solute-solvent systems and appeared to agree well with experimental values. Othmer and Thakar⁽²⁰⁾ offered another correlation by combining Eyring's theory with the Clausius-Claperon equation. Since this correlation has not been thoroughly tested, its validity remains unknown. Diffusivities of electrolytes at infinite dilution can be predicted very accurately by Nernst's equation⁽²¹⁾ while at concentrations other than zero, the equation of Gordon⁽²²⁾ is recommended.

Since no adequately accurate and broadly applicable theory or correlation for the prediction of liquid diffusion^{at higher concentration} exist, experimental techniques have been the main source of diffusion data. Considerable effort and ingenuity has been spent in devising techniques in which variations in concentration, distance, and time can be observed and used in the calculation of the diffusivity from various forms of diffusion equations.

In self diffusion experiments, radioactive isotopes have been extensively used while mutual diffusion measurements have been carried out by a large number of techniques, ranging from a simple diaphragm cell to a sophisticated laser interferometer.

It has been widely agreed that the best combination of simplicity and accuracy is perhaps the method using a diaphragm cell, first introduced by Northrop and Anson⁽²³⁾. In this procedure, the diffusion process takes place through a porous diaphragm connecting two cells in which the respective liquid concentrations are maintained uniform. Convection currents which often occur in large diffusion cells are eliminated because the interfacial areas between 2 liquids are greatly reduced. The diffusivity obtained here represents the integral value of diffusivities in the range of concentrations involved. Though widely used, the diaphragm cell sometimes gives serious differences among data obtained by various investigators. One of the main source of error perhaps lies in the fact that entrapped air or vapor in the porous diaphragm might change the effective diffusion section to a great extent. Furthermore, besides being time consuming, this method also requires that concentrations of solutions interdiffusing must be

small thus rendering the analysis of final solutions inaccurate.

In addition to the diaphragm cell, other devices have been developed such as the capillary cell, the segmented cell, the radioactive cell but so far, the most accurate techniques are the optical cells in which sharp, initial boundary is easy to obtain, changes of concentration with distance and time can be recorded at any time throughout the experiment.

One of the earliest investigators in this optical field was Gouy⁽²⁴⁾ who considered the use of refractive index measurements in diffusivity determination but Wiener⁽²⁵⁾ was the first to be credited with the mathematical formulation of optical diffusion experiments. He developed the equation for the curvature of a light beam passing through a diffusing medium. In Wiener's experiment, curves of refractive index gradient were photographed on a 45° axis and converted to concentration gradient curves. Later, Thovert⁽²⁶⁾ modified this method by photographing Wiener's refractive curve through a cylindrical lens. In this way, curves of concentration gradient were obtained directly in rectangular co-ordinates. With non volatile liquids, another optical method has been used with excellent results: the interferometric method, first presented in 1947 by Kegeles and Gosting⁽²⁷⁾ along with the experimental test of the method of Longworth⁽²⁸⁾. This method was later used by Coulson⁽²⁹⁾, Robinson⁽³⁰⁾ and more recently, by Nishijima and Oster⁽³¹⁾ and Secor⁽³²⁾.

Although very simple and accurate, the interferometric^{method} has at least one disadvantage: the temperature of solutions interdiffusing cannot be controlled easily. To overcome this difficulty, Lamm⁽³³⁾ proposed his well known "scale method" in which displacements of the

marks on a uniformly graduated scale placed between a light source and a diffusion cell were photographed and converted into a concentration gradient curve. In 1964, Sato and co-worker (34) modified this method by putting another screen on the image to make appear a moiré pattern of the refractive index curve. Diffusion coefficients obtained by Sato were often higher than those found by other investigators. The reason of this is that in his experiments, the two solutions interdiffusing were put into contact with each other by pushing the heavier one in under the other solution, thus some convection occurred between the 2 phases at the beginning of the diffusion process. It was the purpose of this project to adopt Sato's method but using an improved cell to obtain accurate diffusion coefficients of binary liquid systems.

3. THEORY

3.1 Derivation of Fick's Second Law

Let us consider an isothermal, free, unidirectional diffusion process between two species A and B along a certain direction x .

3.1.1 Systems with no volume change on mixing

According to Fick's first law, we have, for the species A

$$N_A = -D \frac{\partial c_A}{\partial x} \quad (3.1.1)$$

where N_A is the molar flux of A in the x direction

c_A is its concentration

x is the distance from the boundary, in the diffusion direction

D is the mutual diffusion coefficient between A and B, at the temperature of experiment.

In the absence of chemical reaction between A and B, a balance of material gives us:

$$\frac{\partial c_A}{\partial t} = - \frac{\partial N_A}{\partial x} \quad (3.1.2)$$

Which, combined with (3.1.1), leads to Fick's second law:

$$\frac{\partial c_A}{\partial t} = \frac{\partial}{\partial x} \left(D \frac{\partial c_A}{\partial x} \right) \quad (3.1.3)$$

For dilute solutions, D can be reasonably taken as a constant but in general, it varies with concentration.

Boltzmann⁽³⁵⁾ showed that if c is a function of (x/\sqrt{t}) , as is usually the case, with certain special boundary conditions D can be derived from (3.1.3) as follows:

$$\text{Let } \eta = \frac{x}{\sqrt{t}}$$

We have:

$$\begin{aligned} \frac{\partial c_A}{\partial x} &= \frac{1}{\sqrt{t}} \frac{dc_A}{d\eta} \\ \frac{\partial}{\partial x} \left(D \frac{\partial c_A}{\partial x} \right) &= \frac{\partial}{\partial x} \left(\frac{D}{\sqrt{t}} \frac{dc_A}{d\eta} \right) \\ \frac{\partial}{\partial x} \left(D \frac{\partial c_A}{\partial x} \right) &= \frac{1}{t} \frac{d}{d\eta} \left(D \frac{dc_A}{d\eta} \right) \end{aligned} \quad (3.1.4)$$

and:

$$\frac{\partial c_A}{\partial t} = - \frac{x}{2t} \frac{dc_A}{d\eta} \quad (3.1.5)$$

With these relations, Fick's second law becomes:

$$- \frac{x}{2t} \frac{dc_A}{d\eta} = \frac{1}{t} \frac{d}{d\eta} \left(D \frac{dc_A}{d\eta} \right)$$

or:

$$\eta \frac{dc_A}{d\eta} = -2 \frac{d}{d\eta} \left(D \frac{dc_A}{d\eta} \right) \quad (3.1.6)$$

which is an ordinary differential equation between c and η .

The above transformation can be used when diffusion takes place in infinite media, provided that the concentration is originally constant in the region $x < 0$ and $x > 0$

Thus if:

$$c_A = c_0 \quad \text{for } x < 0 \quad \text{and } t = 0$$

and:

$$c_A = c_1 \quad \text{for } x > 0 \quad \text{and } t = 0$$

the following new boundary condition result:

$$c_A = c_0 \quad \text{for } \eta = -\infty$$

$$c_A = c_1 \quad \text{for } \eta = +\infty$$

An integration of equation (3.1.6) from $c_A = c_0$ to $c_A = c_A$ gives:

$$\int_{c_0}^{c_A} \eta dc_A = -2 \int_{c_0}^{c_A} \frac{d}{d\eta} \left(D \frac{dc_A}{d\eta} \right) d\eta$$

$$\int_{c_0}^{c_A} \eta dc_A = -2 \left[D \frac{dc_A}{d\eta} \right]_{c_0}^{c_A} \quad (3.1.7)$$

Since

$$D \frac{dc_A}{d\eta} \Big|_{c_0} = 0,$$

We have finally:

$$D(c_A) = -\frac{1}{2} \frac{d\eta}{dc_A} \int_{c_0}^{c_A} \eta dc_A \quad (3.1.8)$$

Replacing η by $\frac{x}{\sqrt{t}}$, the above relation becomes:

$$D(c_A) = -\frac{1}{2t} \frac{dx}{dc_A} \int_{c_0}^{c_A} x dc_A \quad (3.1.9)$$

According to these equations, the diffusion coefficient can be calculated as a function of concentration once the concentration profile is available.

Since $D \frac{dc_A}{d\eta} \Big|_{c_1} = 0$ too, from (3.1.7) we have:

$$\int_{c_0}^{c_1} \eta dc_A = \int_{c_0}^{c_1} x dc_A = 0 \quad (3.1.10)$$

To satisfy the boundary conditions, the origin of the x-axis must be determined by (3.1.10).

3.1.2 Systems with Volume Change on Mixing

The interdiffusion of two components forming a system which displays volume change on mixing has been considered by Prager⁽³⁶⁾ and later investigated by Takamatsu and co-workers⁽³⁷⁾ with experiments done on the methanol-water system.

In the case of systems with volume change on mixing, the molar flux of each component can be expressed as following:

$$N_A = -\mathcal{D}_A \frac{\partial c_A}{\partial x} + x_A (N_A + N_B) \quad (3.1.11)$$

$$N_B = -\mathcal{D}_B \frac{\partial c_B}{\partial x} + x_B (N_A + N_B) \quad (3.1.12)$$

where \mathcal{D}_A and \mathcal{D}_B are the intrinsic diffusion coefficients of A and B and x_A , x_B , their mole fractions.

If v is the velocity of the bulk flow, assumed to be in the x-direction and dependent on x and t only, we have:

$$N_A = -\mathcal{D}_A \frac{\partial c_A}{\partial x} + v c_A \quad (3.1.13)$$

$$N_B = -\mathcal{D}_B \frac{\partial c_B}{\partial x} + v c_B \quad (3.1.14)$$

Let \bar{V}_A and \bar{V}_B be the partial molal volumes of A and B. Since only A and B present, at constant pressure and temperature we have:

$$\bar{V}_A c_A + \bar{V}_B c_B = 1 \quad (3.1.15)$$

The definition of a new diffusion coefficient for the diffusion process with volume change on mixing by:

$$D = \mathcal{D}_A \bar{V}_B c_B + \mathcal{D}_B \bar{V}_A c_A \quad (3.1.16)$$

and (3.1.15) can be combined to transform equations (3.1.11) and (3.1.12) to:

$$\frac{\partial c_A}{\partial t} = \frac{\partial}{\partial x} \left(D \frac{\partial c_A}{\partial x} \right) + \frac{\partial}{\partial x} \left\{ c_A \int_{-\infty}^x D g(c_A) \left(\frac{\partial c_A}{\partial x} \right)^2 dx \right\} \quad (3.1.17)$$

and:

$$\frac{\partial c_B}{\partial t} = \frac{\partial}{\partial x} \left(D \frac{\partial c_B}{\partial x} \right) + \frac{\partial}{\partial x} \left\{ c_B \int_{-\infty}^x D g(c_A) \left(\frac{\partial c_A}{\partial x} \right)^2 dx \right\} \quad (3.1.18)$$

where:

$$g(c_A) = \frac{1}{\bar{V}_B c_A} \frac{\partial \bar{V}_B}{\partial c_B} = \frac{(\partial \bar{V}_A / \partial c_A)}{1 - \bar{V}_A c_A} \quad (3.1.19)$$

Details of these transformations can be found in the Appendix I.

With the same boundary conditions as in the first case (i.e. $c = c_0$ for $x < 0$, $t = 0$; $c = c_1$ for $x > 0$, $t = 0$), the Boltzmann variable $\eta = \frac{x}{\sqrt{t}}$ can be used here to give:

$$D(c_A) = -\frac{1}{2} \frac{d\eta}{dc_A} \int_{c_0}^{c_A} \eta dc_A - c_A c_0 \int_{c_0}^{c_A} g(c_A) \left(\int_{c_0}^{c_A} \eta dc_A \right) dc_A \quad (3.1.20)$$

The equation for the determination of the x-origin in this case

is:

$$\int_{c_0}^{c_1} \eta dc_A = c_1 \int_{c_0}^{c_1} g(c_A) \left(\int_{c_0}^{c_1} \eta dc_A \right) dc_A \quad (3.1.21)$$

It should be noted here that in absence of volume change on mixing, $g(c_A) = 0$ and equations (3.1.20) and (3.1.21) reduced to equations (3.1.8) and (3.1.10).

3.2 Relation Between the Moiré Curve and Concentration Gradient

3.2.1 Deflection of a Light Beam Passing Through a Diffusion Cell

The application of optics in diffusion experiments, especially, the observation of deflection of a light beam passing through a medium of varying refractive index, has been treated by Stefan⁽³⁸⁾, Wiener⁽²⁵⁾ and later, by Münter⁽³⁹⁾ and Lamm⁽⁴⁰⁾. The simplest mathematical developments can be summarized as follows⁽⁴¹⁾.

Considering a monochromatic light beam falling perpendicularly upon a medium assumed to be formed by a number of thin layers, each of height Δx , the refractive index n increasing by Δn when we pass from one layer to another, we will have the situation as shown by Figure 1.

The deflection of the light beam when it passes from one layer to the next one is given by the law of refraction:

$$\frac{\sin \psi}{\sin(\psi + \Delta\psi)} = \frac{n + \Delta n}{n} \quad (3.2.1)$$

If Δx is small enough, we have:

$$\frac{\sin \psi}{\sin \psi + \Delta\psi \cos \psi} \approx \frac{n + \Delta n}{n} \quad (3.2.2)$$

or:

$$-(\cotan \psi) \Delta\psi \approx \frac{\Delta n}{n} \quad (3.2.3)$$

If y is the direction of the light beam, from Fig. 1, we have:

$$\Delta x = \Delta y \cotan \psi \quad (3.2.4)$$

And from (3.2.3) and (3.2.4):

$$\frac{\Delta\psi}{\Delta y} \approx - \frac{\Delta n}{n\Delta x} \quad (3.2.5)$$

On the other hand, the radius of curvature of the deflected light is:

$$\rho = \frac{1}{d\psi/dy} \quad (3.2.6)$$

When Δy is very small, we have:

$$\rho \approx \frac{n}{dn/dx} \quad (3.2.7)$$

This is the relation between the radius of curvature of a deflected light beam, the refractive index and the refractive index gradient.

Let us now see how the above relation can be applied in diffusion measurements.

Considering a diffusion cell which consists of two thin, transparent glass plates S_1 , S_2 and which contains a medium of continuously changing refractive index (Fig. 1).

If a is the width of the cell, b is the distance from it to a screen where a deflection z of the original light beam is recorded, we shall have (for $a \ll b$):

$$z \approx b\theta_2 \quad (3.2.8)$$

θ_2 : angle of deflection of the light beam when it emerges from the cell.

If n' is the refractive index of the medium surrounding the diffusion cell, we have:

$$n'\theta_2 \approx n\theta_1 \quad (3.2.9)$$

with θ_1 , as the incident angle of the light beam on surface S_2 .

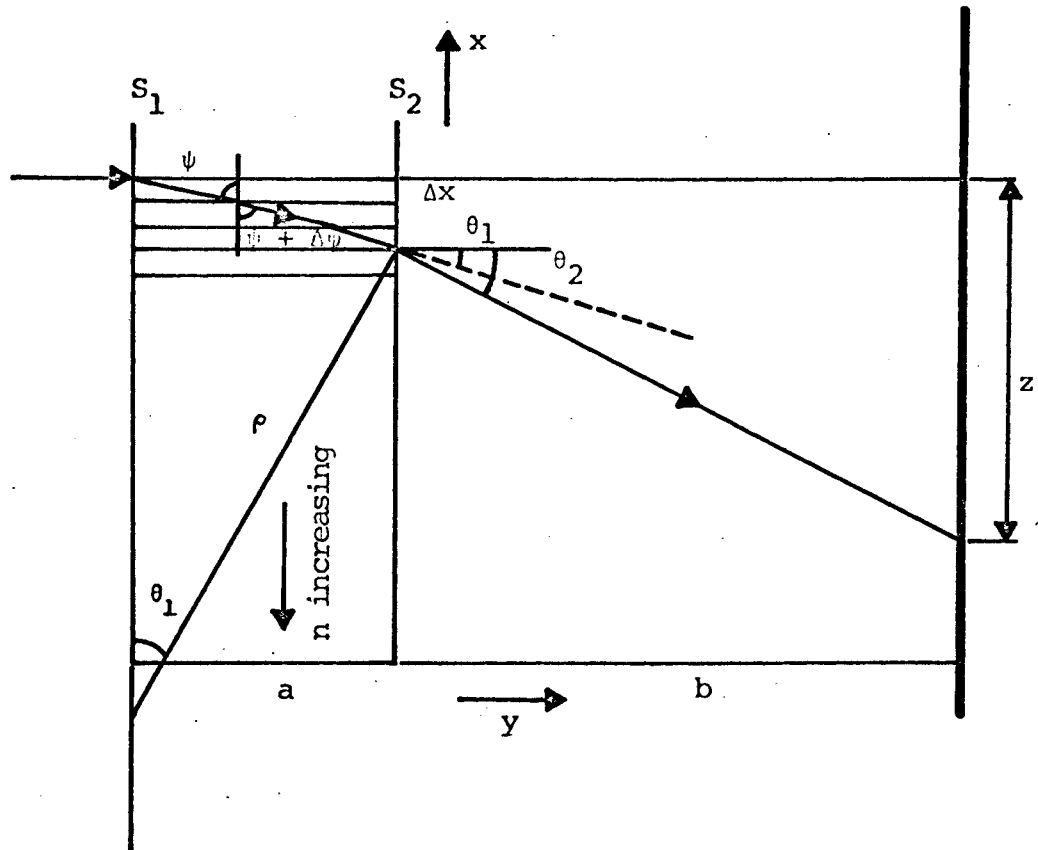


Figure 1

Deflection of a light beam passing through a medium of continuously varying refractive index

Moreover,

$$\theta_1 \approx \frac{a}{\rho} \quad (3.2.9)$$

from the definition of the radius of curvature of the deflected light beam.

The three previous expressions can be combined to give:

$$z \approx \frac{nab}{n\rho} \quad (3.2.10)$$

Replacing ρ by $-\frac{n}{dn/dx}$, we obtain:

$$z \approx -\frac{ab}{n'} \frac{dn}{dx} \quad (3.2.11)$$

or, in absolute value,

$$z \approx \frac{ab}{n'} \frac{dn}{dx} \quad (3.2.12)$$

This is the expression of the deflection of the light beam in terms of the width of the cell, the distance from the cell to the screen where the deflection is recorded and the refractive index gradient.

3.2.2 Height of the Moiré Curve and Concentration Gradient

In Fig. 2a, (A) is a glass grating screen with parallel, equidistant lines; (B) is a diffusion cell where the refractive index gradient exists in the vertical direction only. The lines on (A) are put perpendicular to the direction of diffusion in (B).

When a parallel light beam is directed through the screen and the cell, an image (C) of (A) which can be observed in front of the cell, consists of a series of parallel but non-uniformly spaced lines. The displacement of any line from (A) to (C) is given by equation (3.1.12) if (C) is far enough from (B). If the displacements of the lines are plotted against the position of the original lines, the refractive index

gradient curve will be obtained. This method is the well-known Lamm scale method (39).

Sato and Miyamoto have shown⁽⁴²⁾ that if another screen (D), the same as (A), is placed upon (C) so that the lines of (D) make a small angle with those of (C), moiré curves⁽⁴³⁾ will appear: it is the refractive index curve, same as the curve obtained by Lamm's scale method but can be observed directly.

The geometry of the moiré curves can be explained as follows:

In Fig. 2b, (A) and (D) - two screens with parallel lines spaced at a distance d - make a small angle ϕ between them. The image (C) of (A) is represented by the dash lines.

When the concentration of the medium inside the diffusion cell is uniform (i.e. no mutual diffusion), straight lines like l_1, l_2 , will not be straight. They bend because the images of lines on (A) are not uniformly spaced.

Let us consider a point P on l_1 . Because of the deflection of the light beam passing through the screen (A) and the cell, a line on (A) passing through P will have an image on (C) a line passing through P'. Let z be the vertical distance between these two lines.

If:

$$PP' = u,$$

we have:

$$u = \frac{z}{\sin\phi} \quad (3.2.13)$$

but according to (3.2.12),

$$z = \frac{ab}{n'} \frac{dn}{dx}$$

Thus:

$$u = \frac{ab}{r\sin\phi} \frac{dn}{dx} \quad (3.2.14)$$

where a is the width of the cell, b is the distance from the cell to (D).

Now if it is assumed that the refractive index is a linear function of concentration, as is usually the case, we can write:

$$n = n_0 + kc \quad (3.2.15)$$

Where n_0 is the refractive index of the solvent, k is a constant of proportionality, and c is the concentration of the solute.

Equation (3.2.14) and (3.2.15) can be combined to give:

$$u = \left(\frac{abk}{r\sin\phi}\right) \frac{dc}{dx} \quad (3.2.16)$$

In a system where a , b , k and ϕ are fixed, we have:

$$u = K \frac{dc}{dx} \quad (3.2.17)$$

Where K is another constant of proportionality, equal to

$$\frac{abk}{r\sin\phi}.$$

At this point, it can be stated that the height of moiré curves along the direction of the lines on (D) is proportional to the refractive index gradient.

Equation (3.2.17) will be used to plot the concentration gradient curve ($K \frac{dc}{dx}$ vs. x) to determine the concentration profile and to calculate diffusion coefficients according to equations (3.1.8), (3.1.9) or (3.1.20), depending on the case.

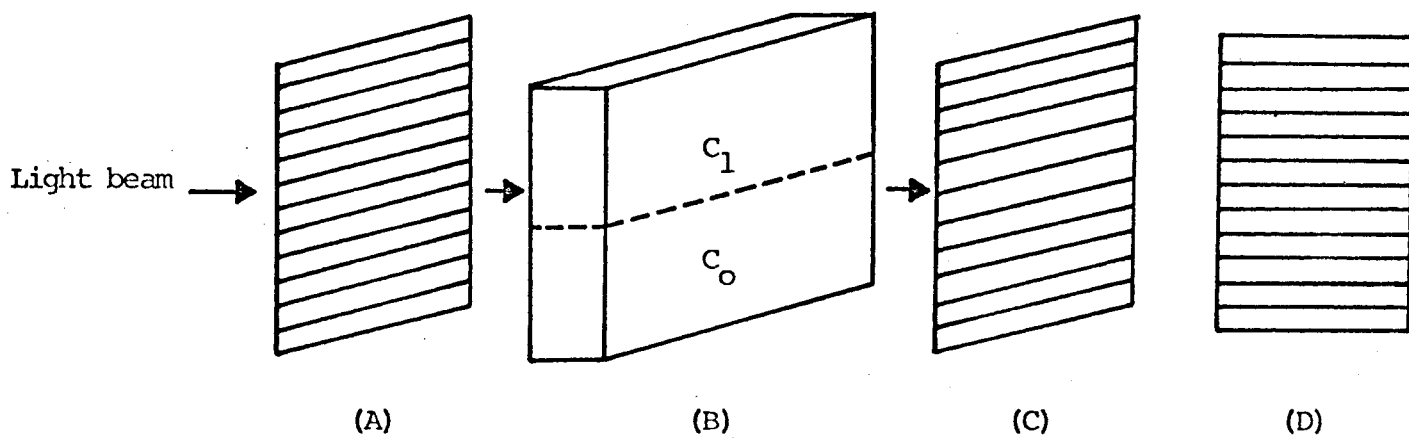


Figure 2a

Disposition of the diffusion cell and the screens

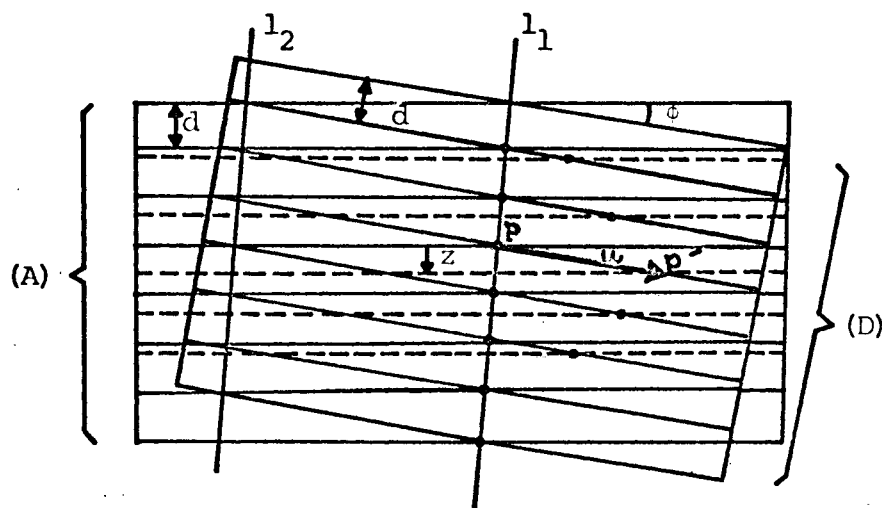


Figure 2b

Relation between height of moiré curves and refractive index gradient

4. Experiments

4.1 Apparatus

4.1.1 The Diffusion Cell (Fig. 3a)

The diffusion cell consists mainly of two parts: a Teflon block (I) reinforced by a stainless steel case and a stainless steel body (II). The Teflon block (I) can be moved horizontally in (II) by a lever (III). A steel plate, placed on the top of (I) can be pressed downward by two bolts to keep the Teflon block in tight contact with the steel body.

Both sides of (II) are mounted with optically flat glass plates, fixed by two screw-tightened windows. To prevent water of the temperature-controlled bath from leaking to the cell, rubber gaskets are placed between the windows and the main body and also, between the windows and the glass plates.

The whole cell measures 12.7 cm high, 8.3 cm wide and 2.5 cm thick. The test sections in the Teflon block (I) and the steel body (II) are both 2 cm high and 1 cm wide.

4.1.2 Experimental Setup

The experimental setup is shown in Fig. 3b. The diffusion cell is placed inside a two-window bath (a) which temperature is controlled by a thermostat (Haake unit). Light beam, from a point source (b) (Sylvania concentrated arc lamp K25) cast through a collimator lens (c) becomes parallel and passes through the windows of the water bath and the diffusion cell. The image of the screen (d) (with horizontal, uniformly spaced lines), superimposed by the screen (e) appears on a

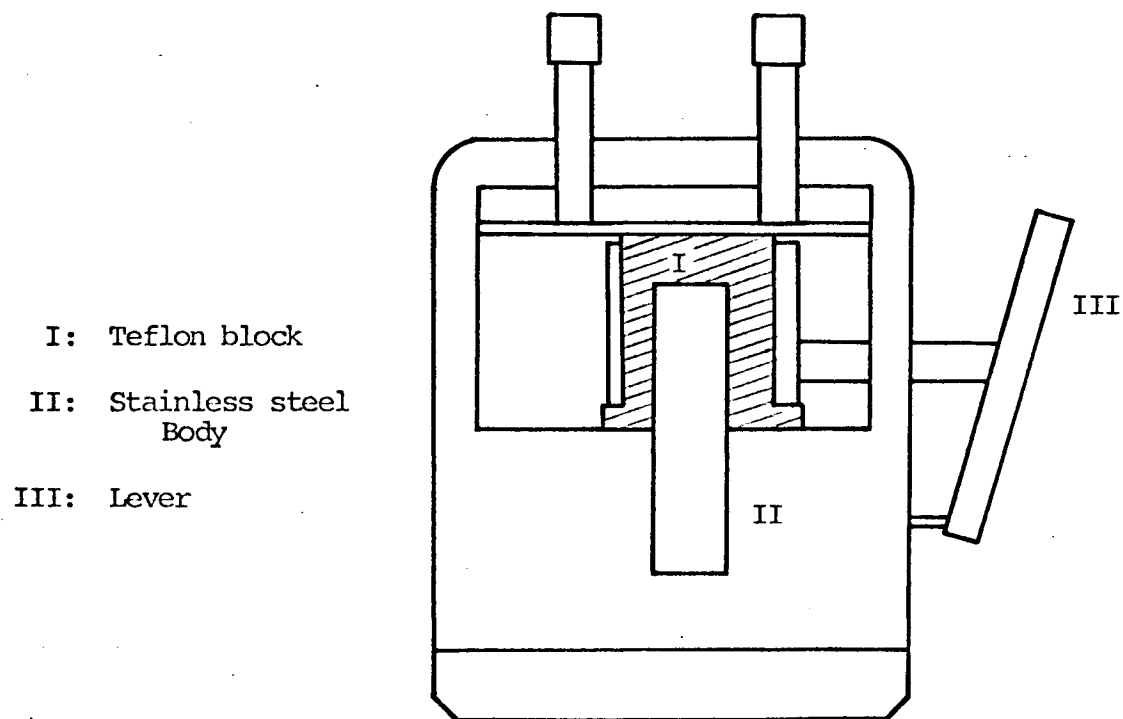


Figure 3a

The Diffusion Cell

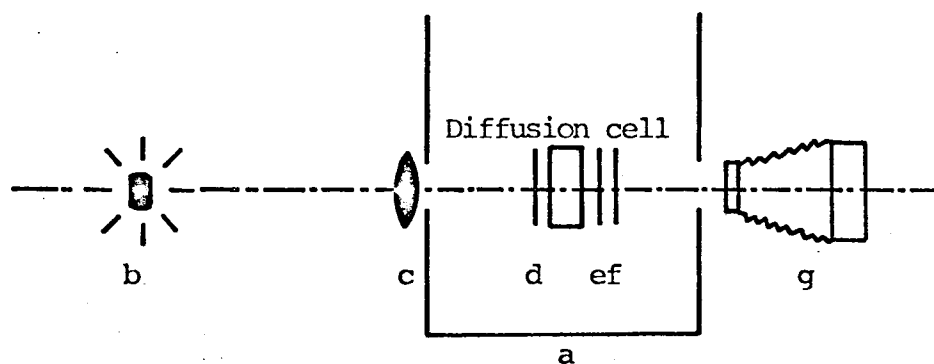


Figure 3b

Experimental setup

ground glass (f) and is photographed by a Pentax Camera (g) (Model S1) equipped with a close up extension tube (No. 2). The settings on the camera are: f4 and $\frac{1}{2}$ second with Isopan ISS film.

4.1.3 Refractive Index Measurements

Refractive indexes of all systems investigated were measured as a function of concentration with a dipping refractometer (Bauch and Lomb Co.) at controlled temperatures ($\pm 0.1^{\circ}\text{C}$).

4.2 Procedure

At the beginning of the experiment, all parts of the diffusion cell are cleaned with soap, chromic acid, rinsed with double-distilled water then, dried in air. After the cell is reassembled, the Teflon block is placed at position 1 - Fig. 4a. The heavier of the two solutions interdiffusing is then injected to the lower compartment and the other one, to the upper part of the test section with a 5 cc hypodermic syringe.

The cell is now placed inside the temperature controlled bath. To start the experiment, the Teflon block is slowly pushed to position 2 - (Fig. 4a) by means of the lever. Both sides of the Teflon block are then filled up with the lighter solution to equalize the hydrodynamic pressures inside and outside the test section.

The timer is started when one half of the lower compartment is overlapped by the upper one. Finally, the light source is turned on and photographs are taken at different times (e.g. every 10 minutes over 5 hours for the sucrose-water system).

After developing the film with D76 developer, the moiré curves on the negative are magnified through a microfilm reader and traced out.

Prior to the experiment itself, refractive indices of the system are measured at various concentrations to make sure that the relation between them is a linear one.

4.3 Method of Calculation

Suppose that from the picture, the curve in Fig. 4b is obtained, with U as the direction of the lines on the second screen (e).

First of all, heights $u (= K \frac{dc_A}{dx})$ of the moiré curve are measured at different points on the x-axis and reconstructed to give the concentration gradient curve (Fig. 5a).

At the point M, the concentration of A is c_1 (solvent side or solution of lower concentration) and at the point N, it is c_0 (solution of higher concentration).

If we integrate the surface under the $K \frac{dc_A}{dx}$ vs. x curve from M to N, we have:

$$\int_{-\infty}^{+\infty} K \frac{dc_A}{dx} dx = \int_{c_1}^{c_0} K dc_A = K (c_0 - c_1) = S \quad (4.3.1)$$

At a certain value the x abscissa, we have:

$$\int_{-\infty}^x K \frac{dc_A}{dx} dx = \int_{c_1}^{c_A} K dc_A = K (c_A - c_1) = s \quad (4.3.2)$$

Dividing (4.3.2) by (4.3.1), the following relation is obtained:

$$\frac{s}{S} = \frac{c_A - c_1}{c_0 - c_1} \quad (4.3.3)$$

Thus if s and S are given by a numerical integration, we can determine the concentration c_A at any point along the x-axis.

In the case of diffusion between a solvent and a solution of concentration c_0 , we have: $c_1 = 0$

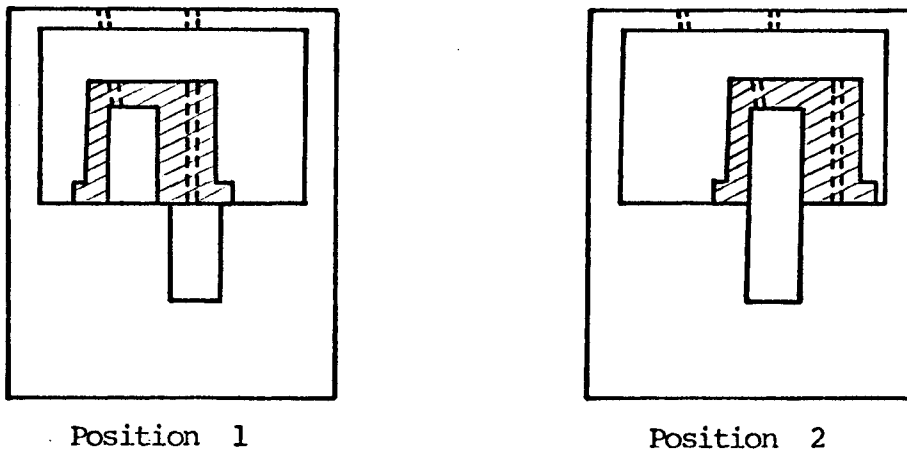


Figure 4a

Procedure

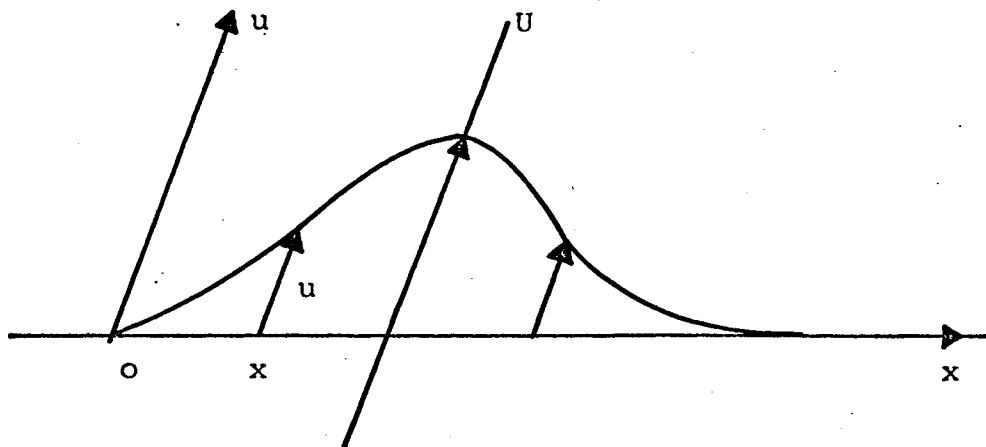


Figure 4b

Moiré curve and Concentration Gradient Profile

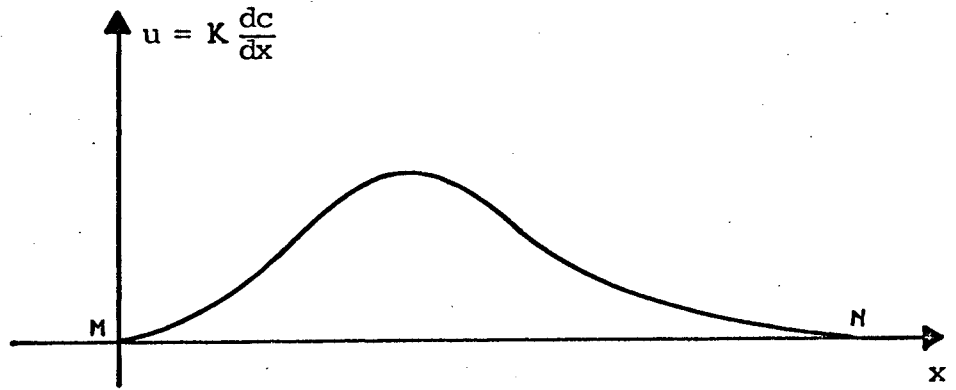


Figure 5a

Integration of moiré curves

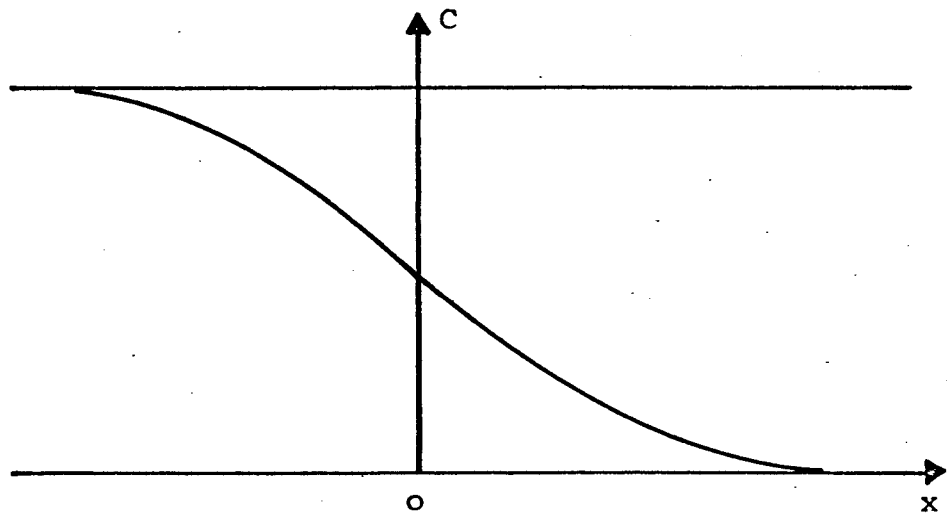


Figure 5b

Concentration Profile with corrected x-origin

Hence:

$$c_A = \frac{s}{S} c_0 \quad (4.3.4)$$

Once the concentration profile of the system has been established Fick's second law is used to calculate the diffusion coefficient according to equation (3.1.8), (3.1.9) or (3.1.20).

Since in Fick's equations, x is in the direction of diffusion, i.e. from a more concentrated solution to a less concentrated solution, we plot the concentration profile as shown by Fig. 5b.

To find the origin of the x -axis, equation (3.1.10) or (3.1.21) is used, with the help of the Fibonacci root searching technique.

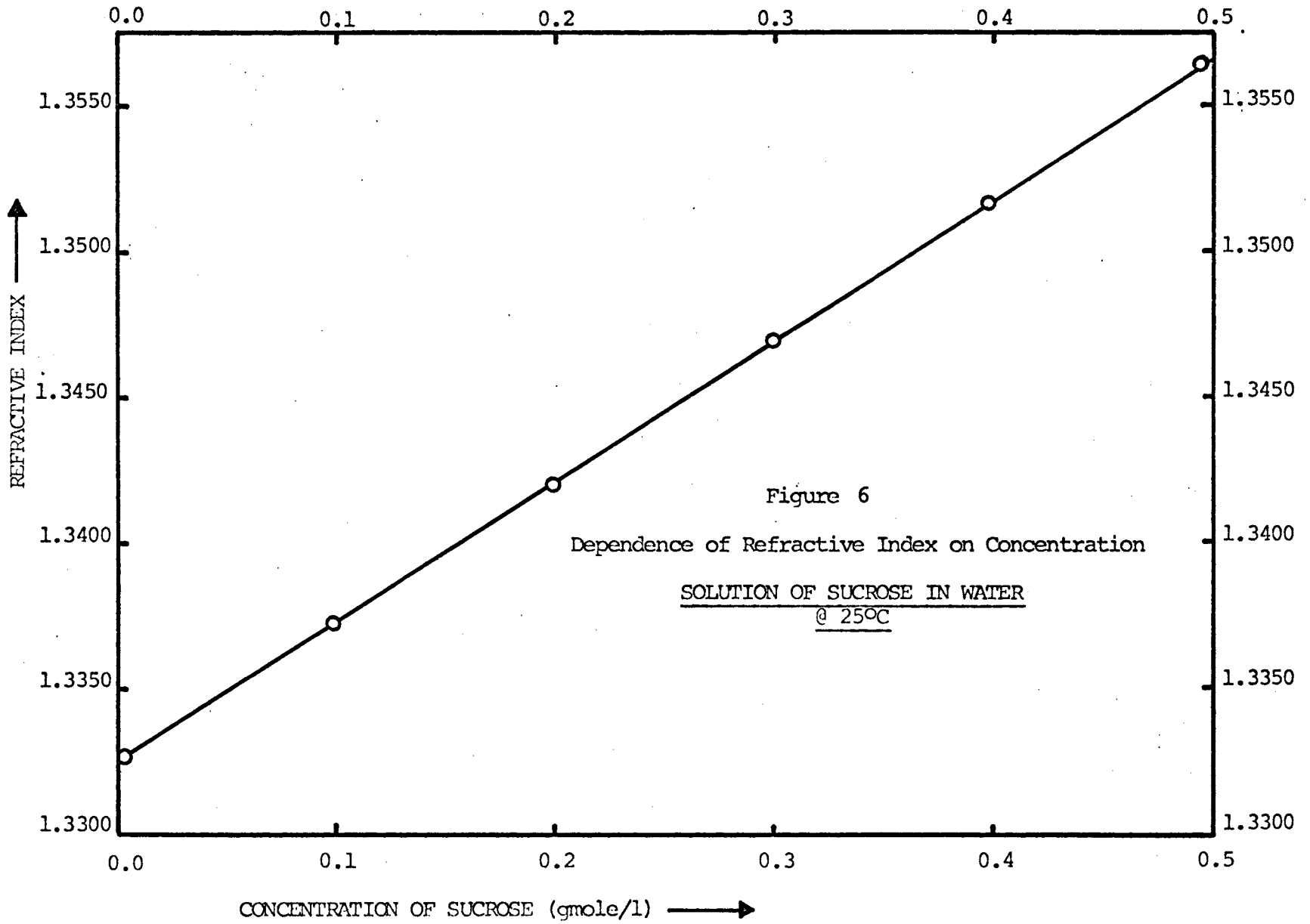
All the calculations involved in this project have been programmed and run with an IBM 7040 computer. The programs can be found in the Appendix III.

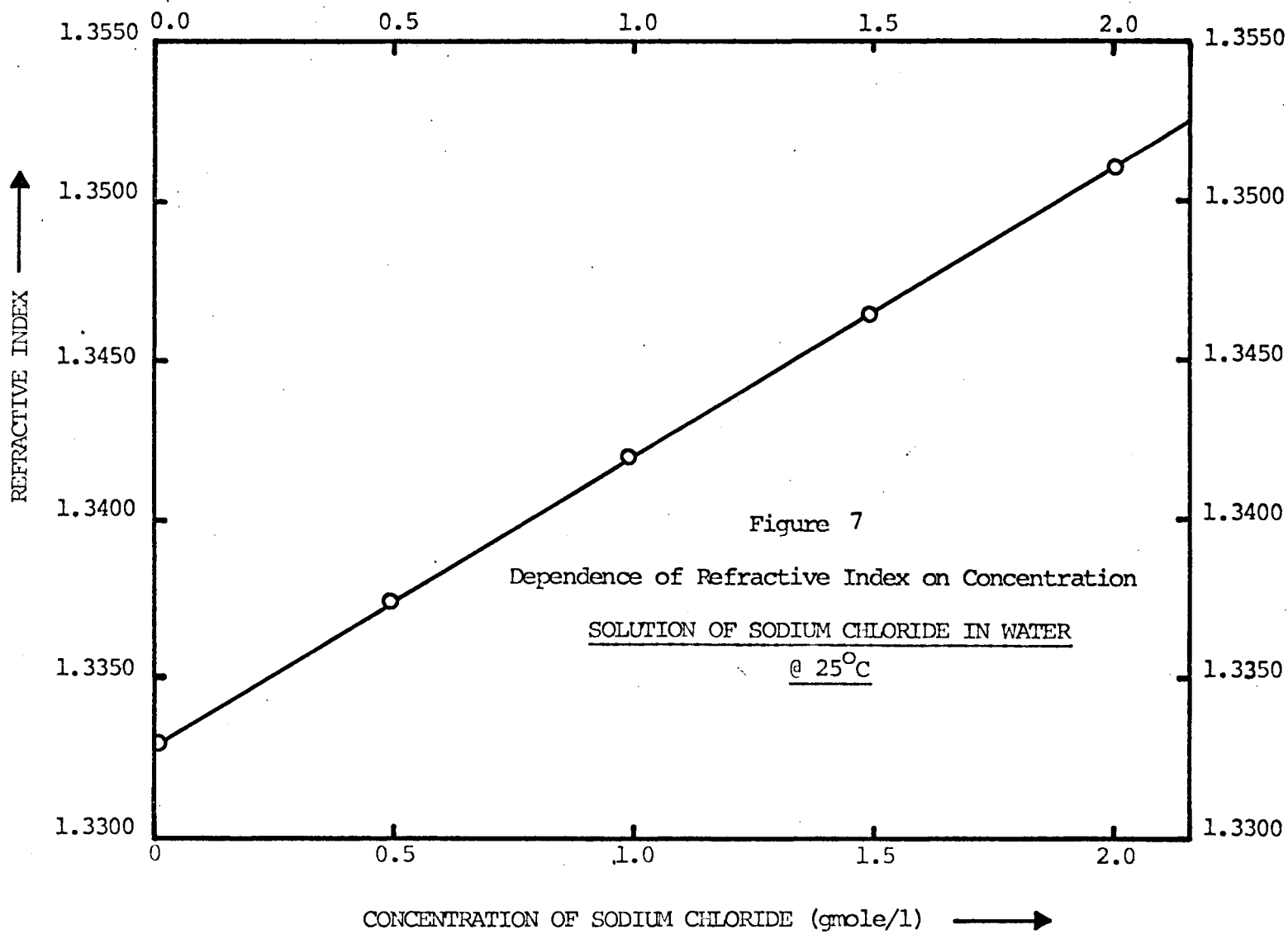
5. Results

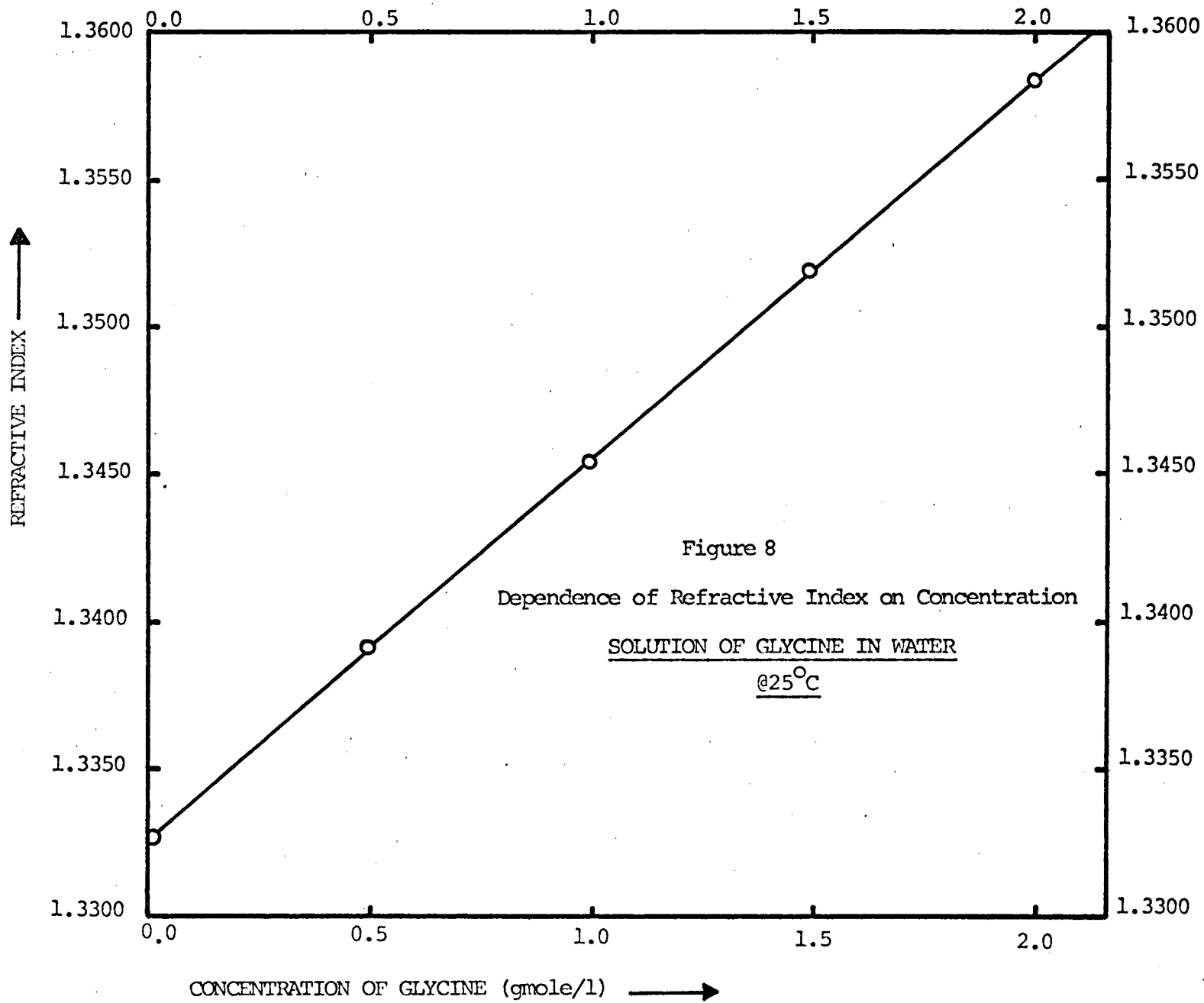
Diffusion coefficients of 5 inorganic and organic systems have been measured - all at 25°C. The reason for this choice of temperature is that data of the investigated systems are all available at 25°C, allowing a comparison of results and evaluation of the moiré pattern method.

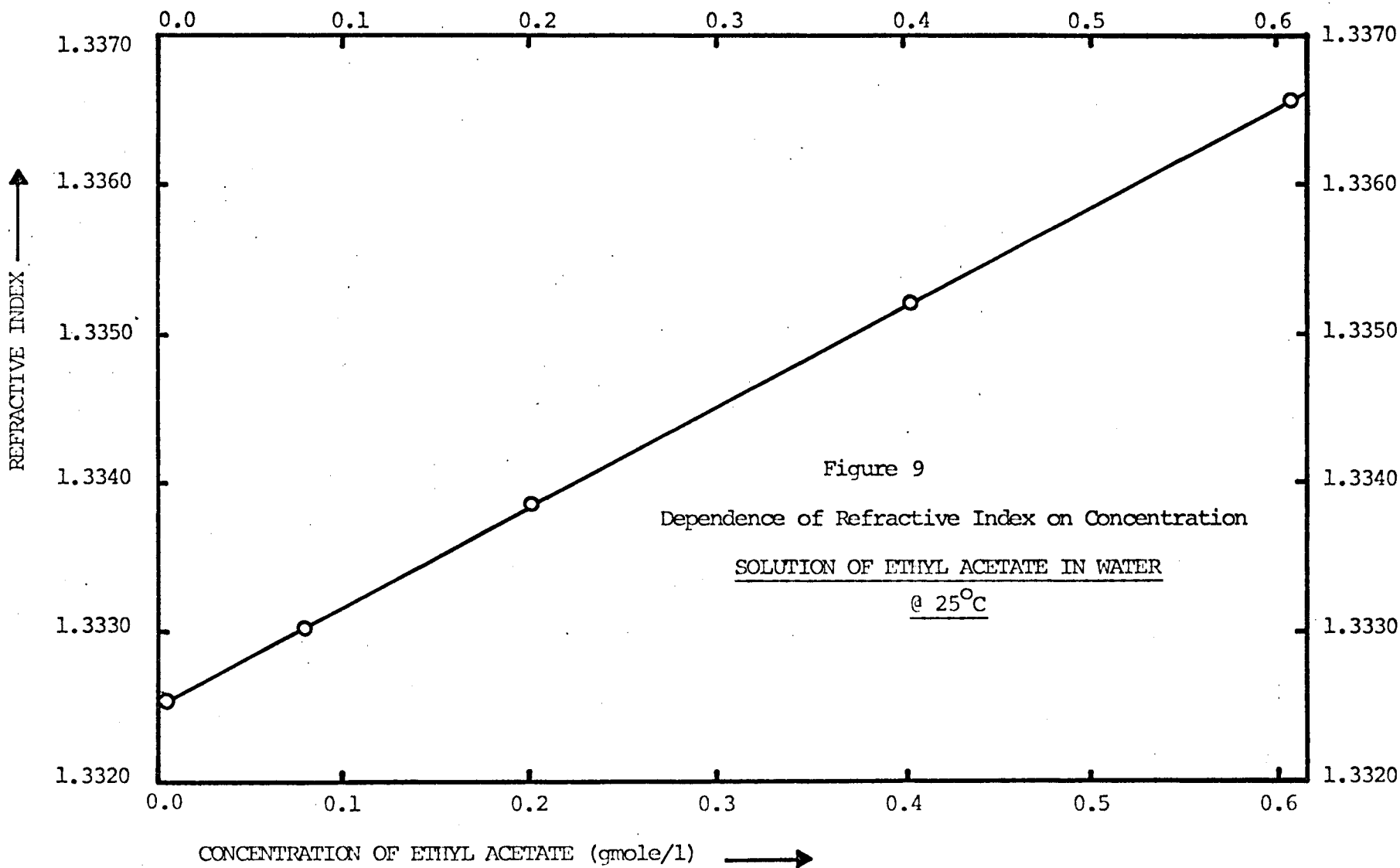
Refractive index data of the systems used were obtained first to check the linear dependence of refractive index on concentration. These data are shown in Fig. 6, 7, 8, 9, and 10.

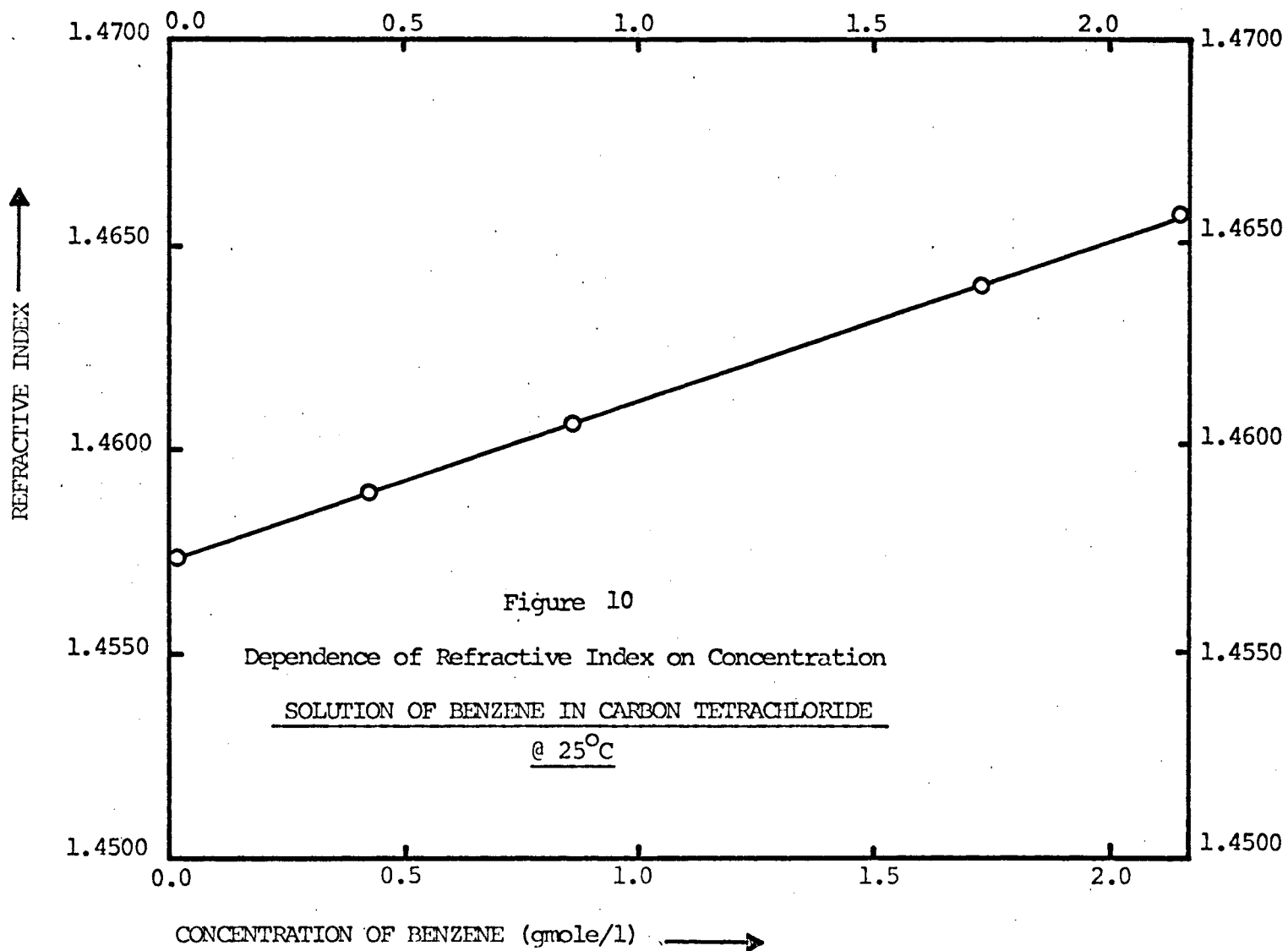
As for the experiments themselves, four runs have been done for each system and two photographs of each run were analyzed to calculate diffusivities. That is, 8 sets of results were obtained for each system. A regression analysis was then applied to find by the least square









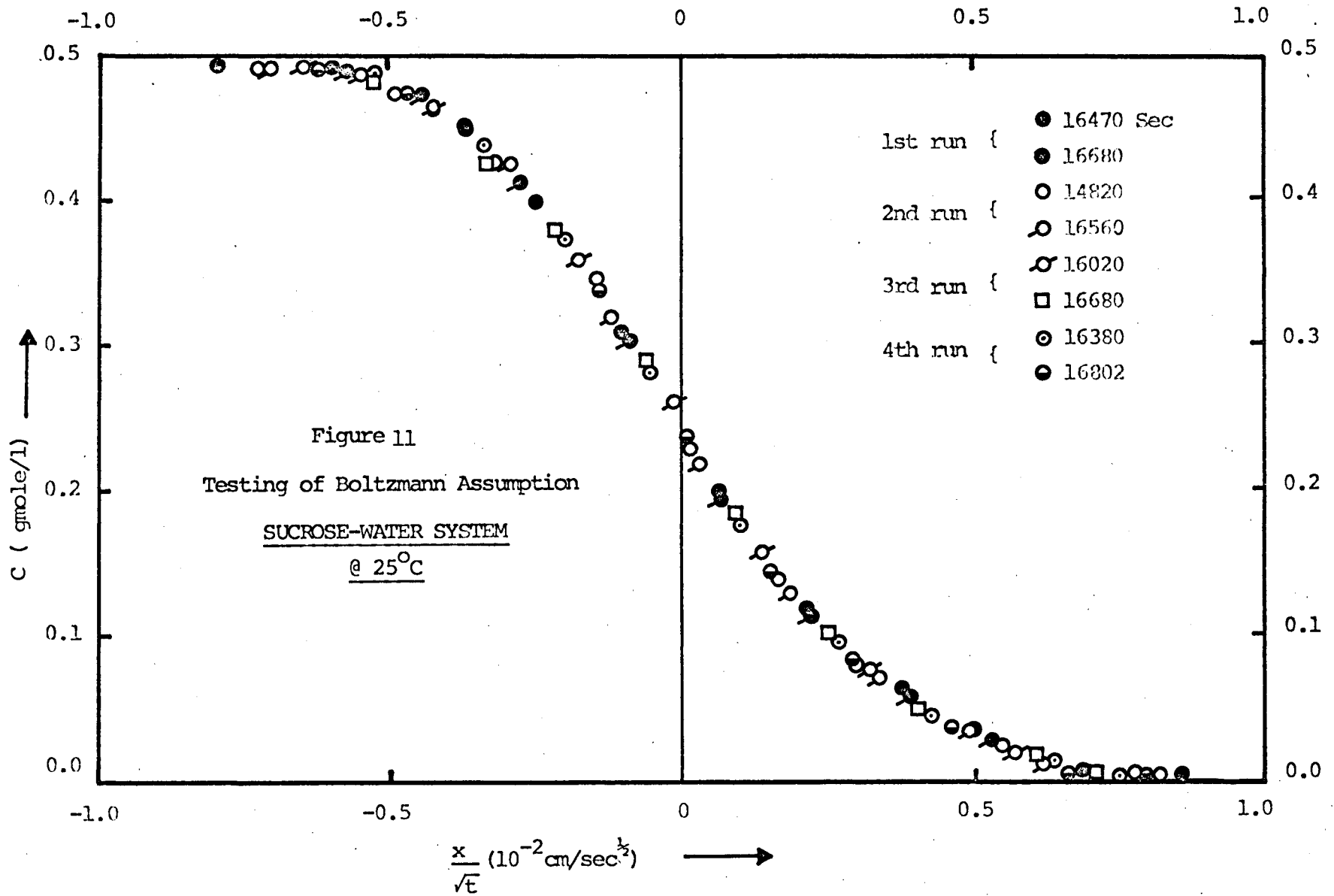


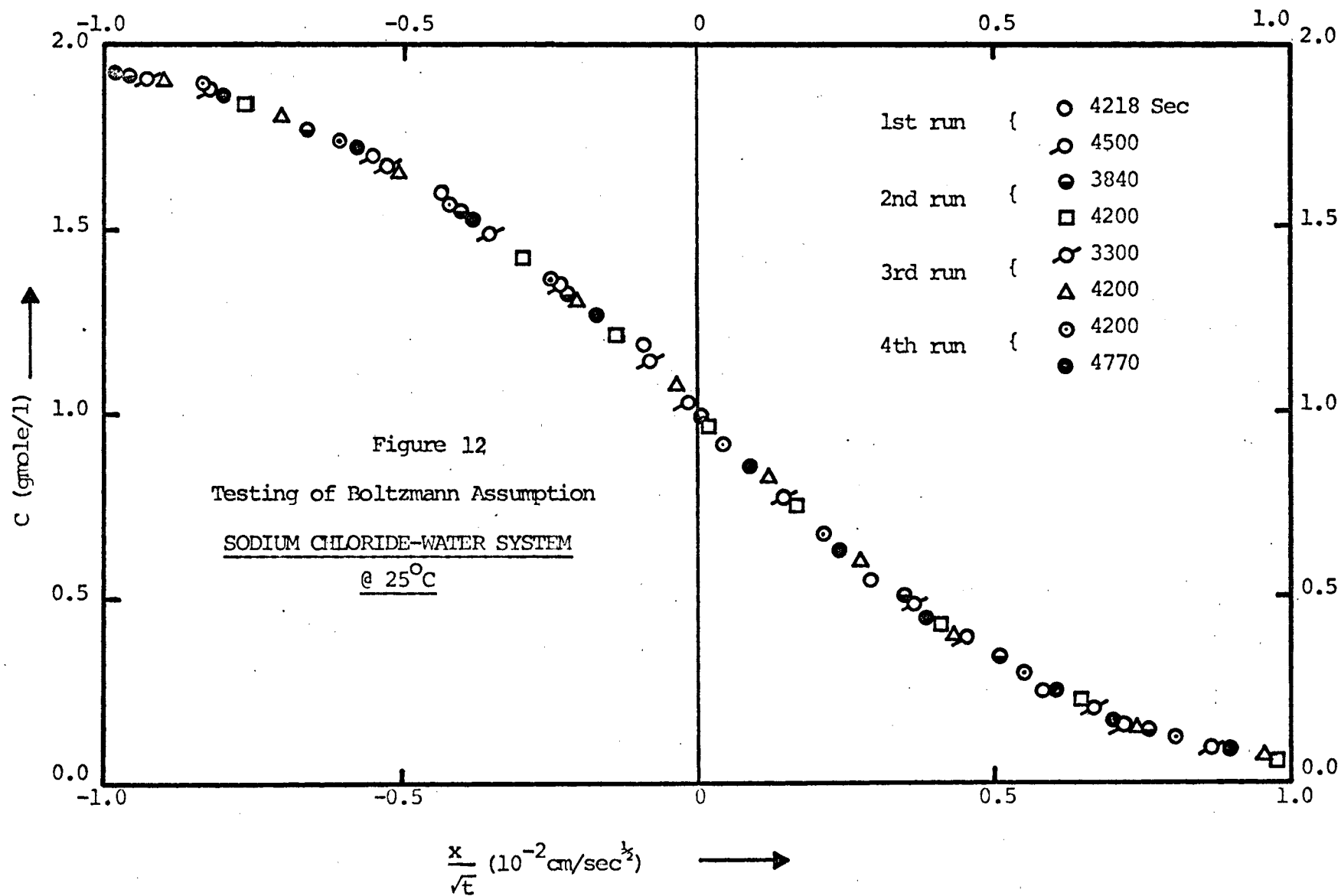
method, the polynomial which best fits the experimental data of each system.

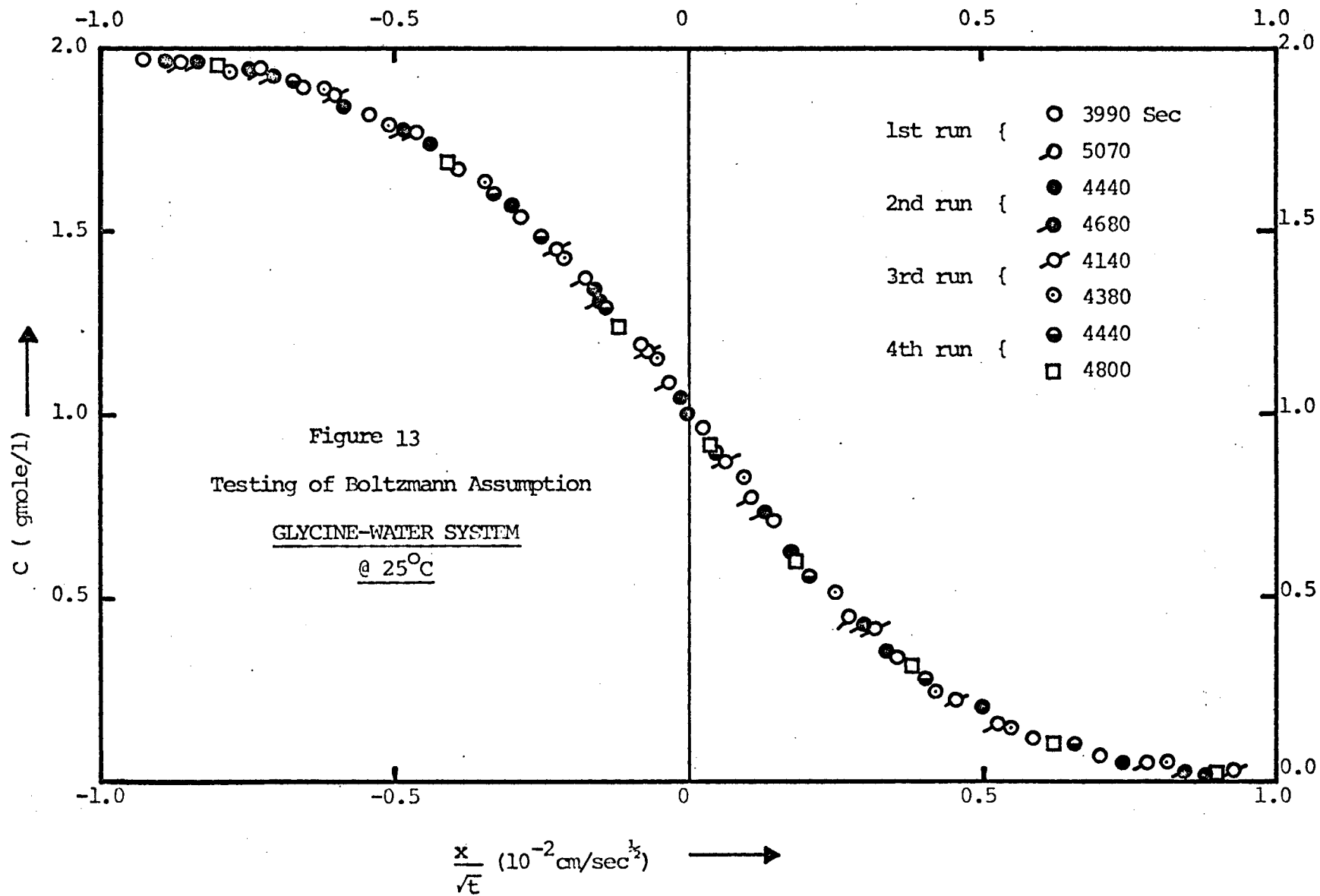
In the following table solution 1 and solution 2 represent the two solutions interdiffusing. The third column represents the original concentration of solution 2 according to which diffusivities were calculated, the original concentration of solution 1 being zero for all systems (pure solvent). These concentrations have been chosen since diffusion coefficients of the investigated systems are available at these concentrations, thus a comparison of results is possible.

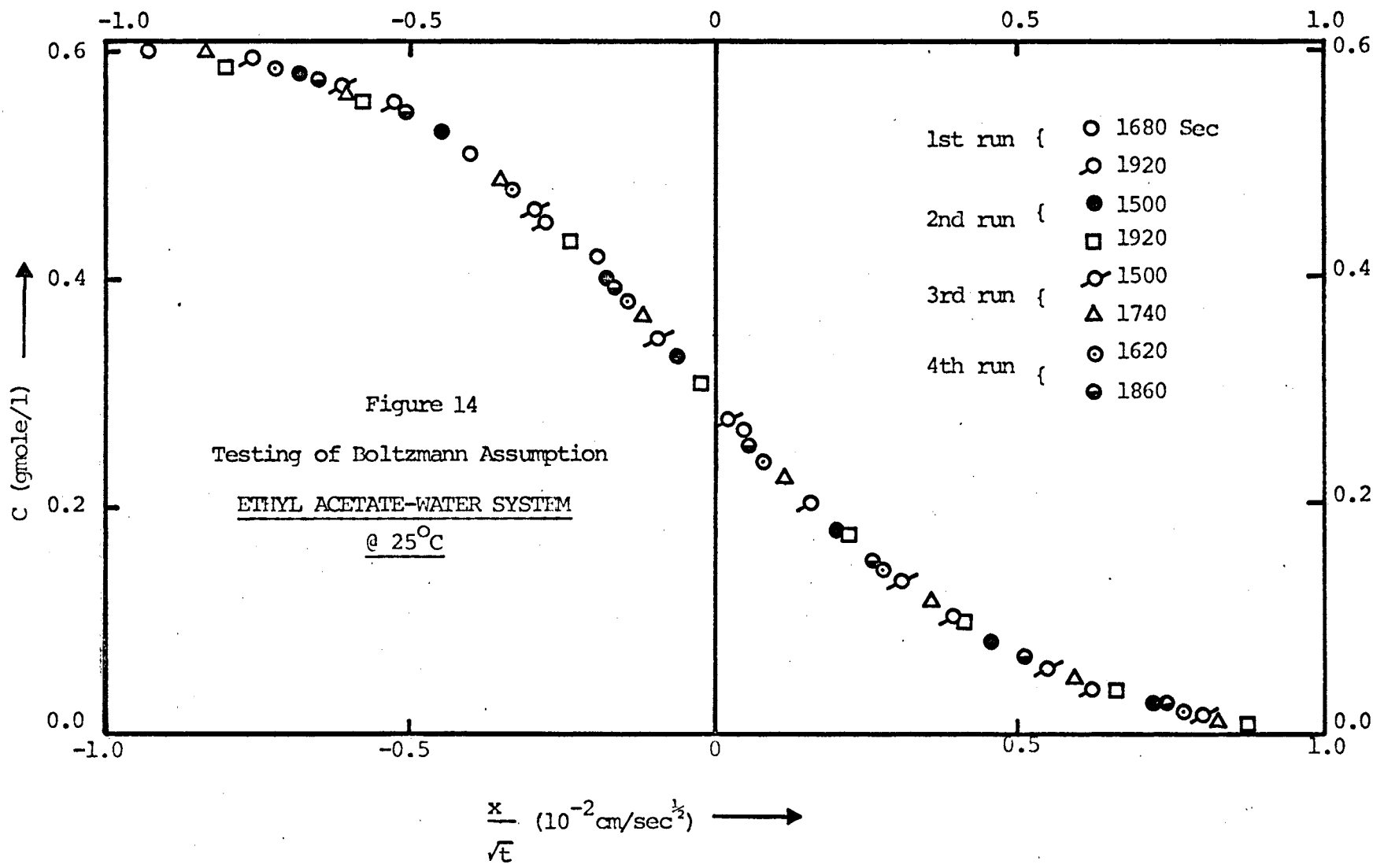
Solution 1	Solution 2	Concentration of 2 (gmole/l)
Water	Sucrose	0.500
Water	Sodium Chloride	2.000
Water	Glycine	2.000
Water	Ethyl Acetate	0.608
Carbon Tetrachloride	Benzene	2.012

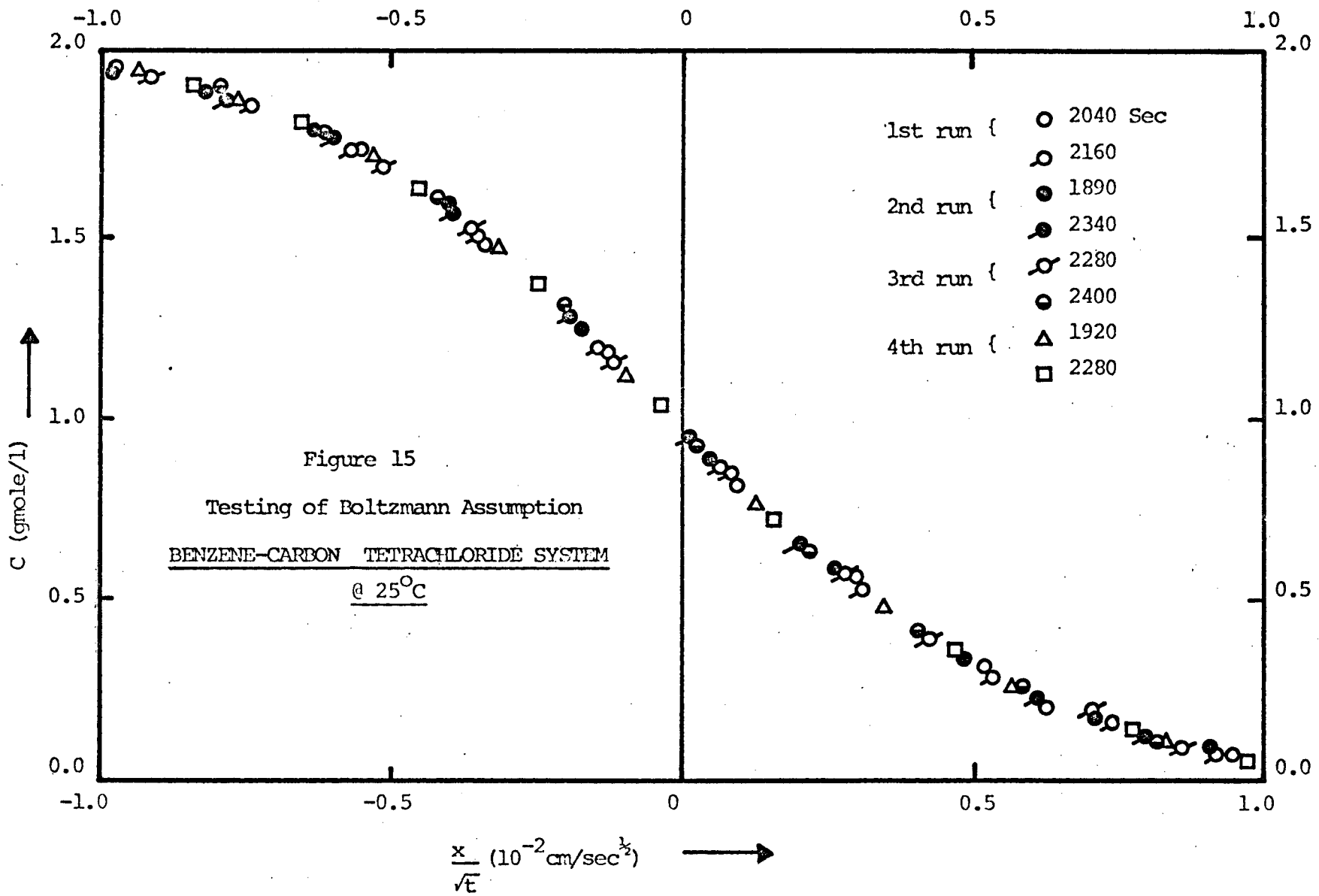
The Boltzmann assumption ($c = f(x/\sqrt{t})$) was tested in each case to make sure that the concentration profile for each system can be represented by a unique curve of c vs. x/\sqrt{t} . These curves are shown in Fig. 11, 12, 13, 14 and 15.











It should be here added that all the systems considered in this project were supposed to have no volume change on mixing, they were considered to be nearly ideal because either they display no volume change or because the concentrations involved were small (ethyl acetate - water, benzene-carbon tetrachloride systems). Thus, in the calculations equations (3.1.9) and (3.1.10) were used.

Curves of diffusivities vs. concentrations are shown in Fig. 16, 17, 18, 19 and 20.

To test the method of calculation used here, a computer program was prepared to predict the concentration profile from the expression of diffusion coefficient in function of concentration found for each system.

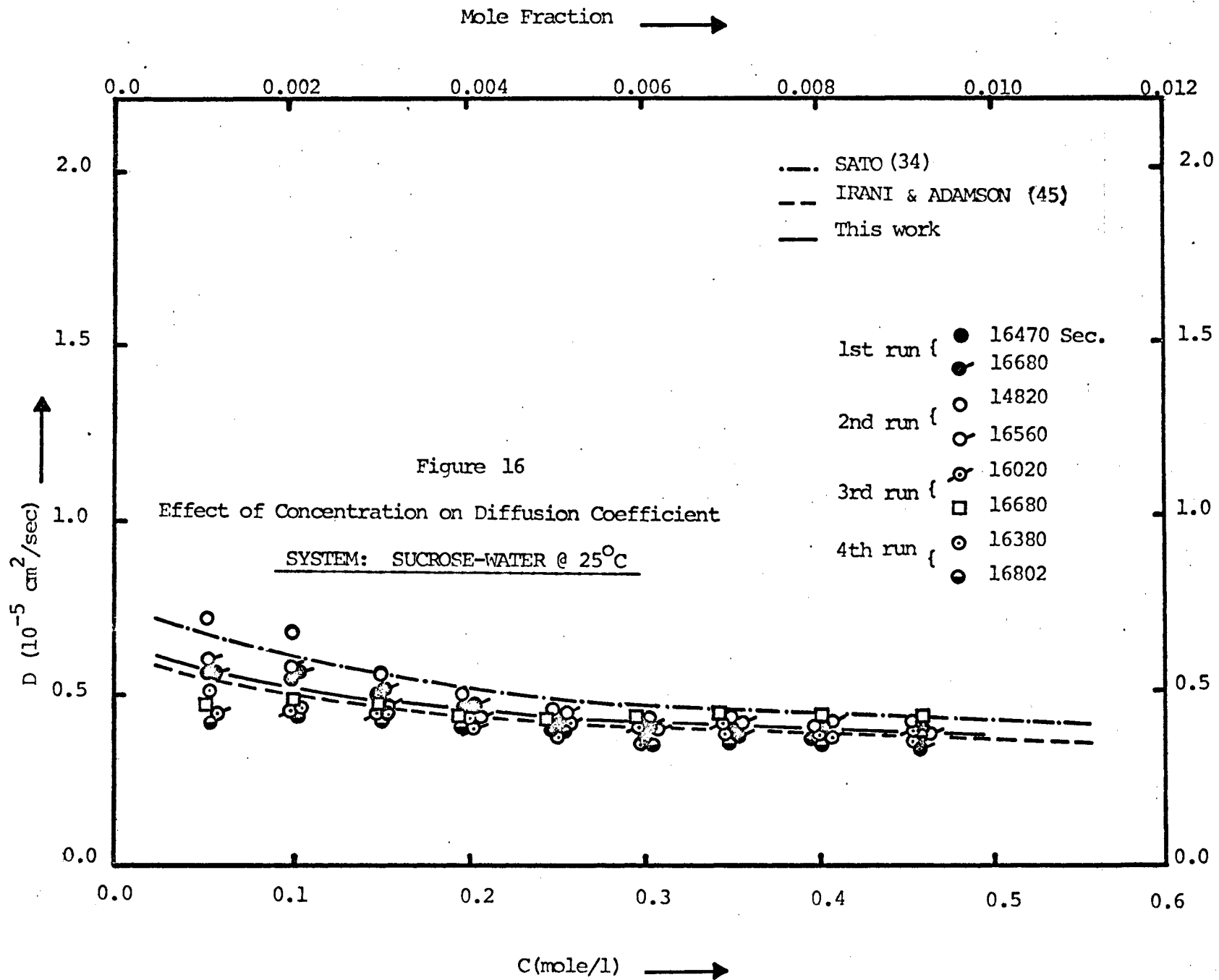
In order to use Fick's second law:

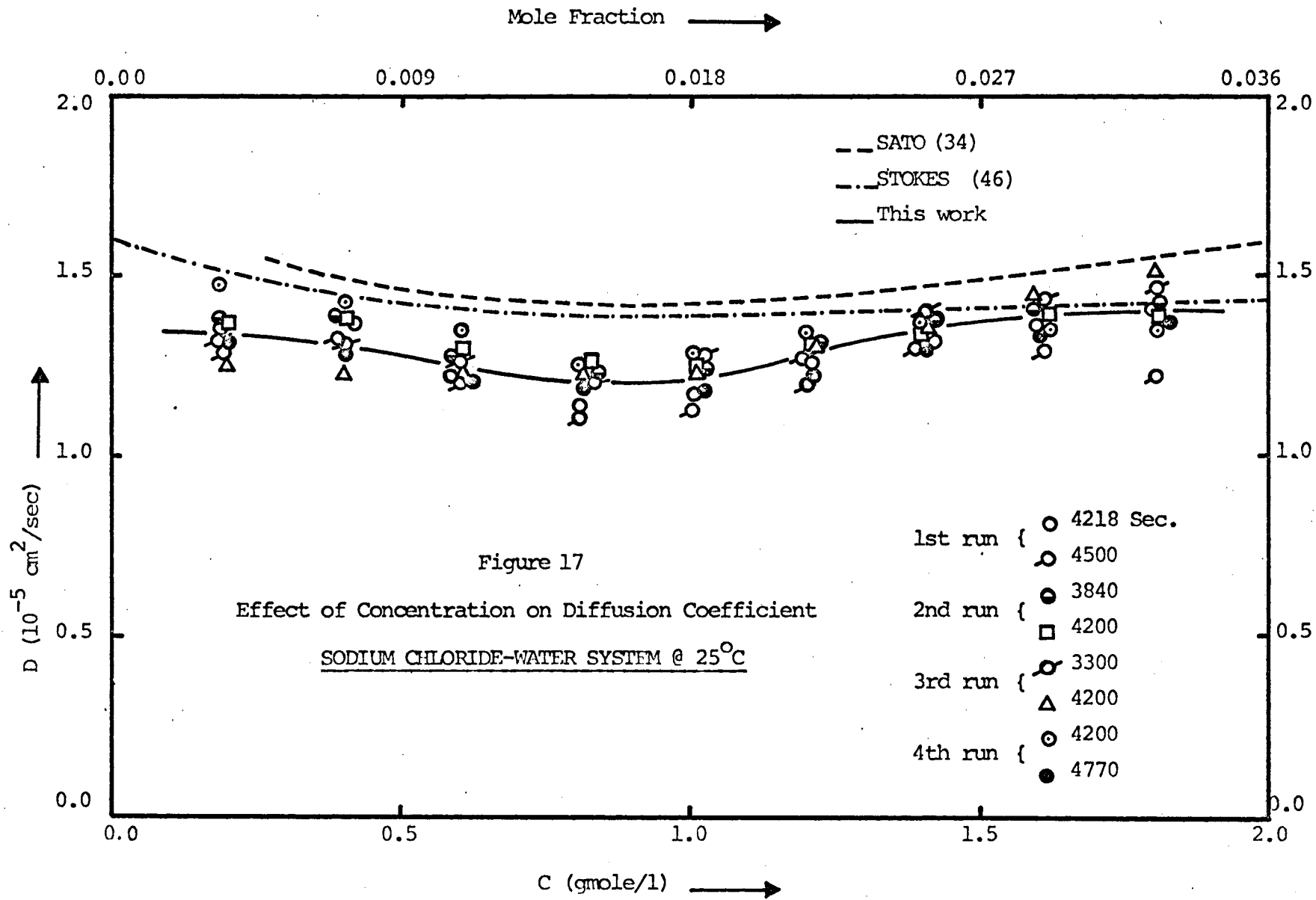
$$\frac{\partial c}{\partial t} = \frac{\partial}{\partial x} \left(D \frac{\partial c}{\partial x} \right)$$

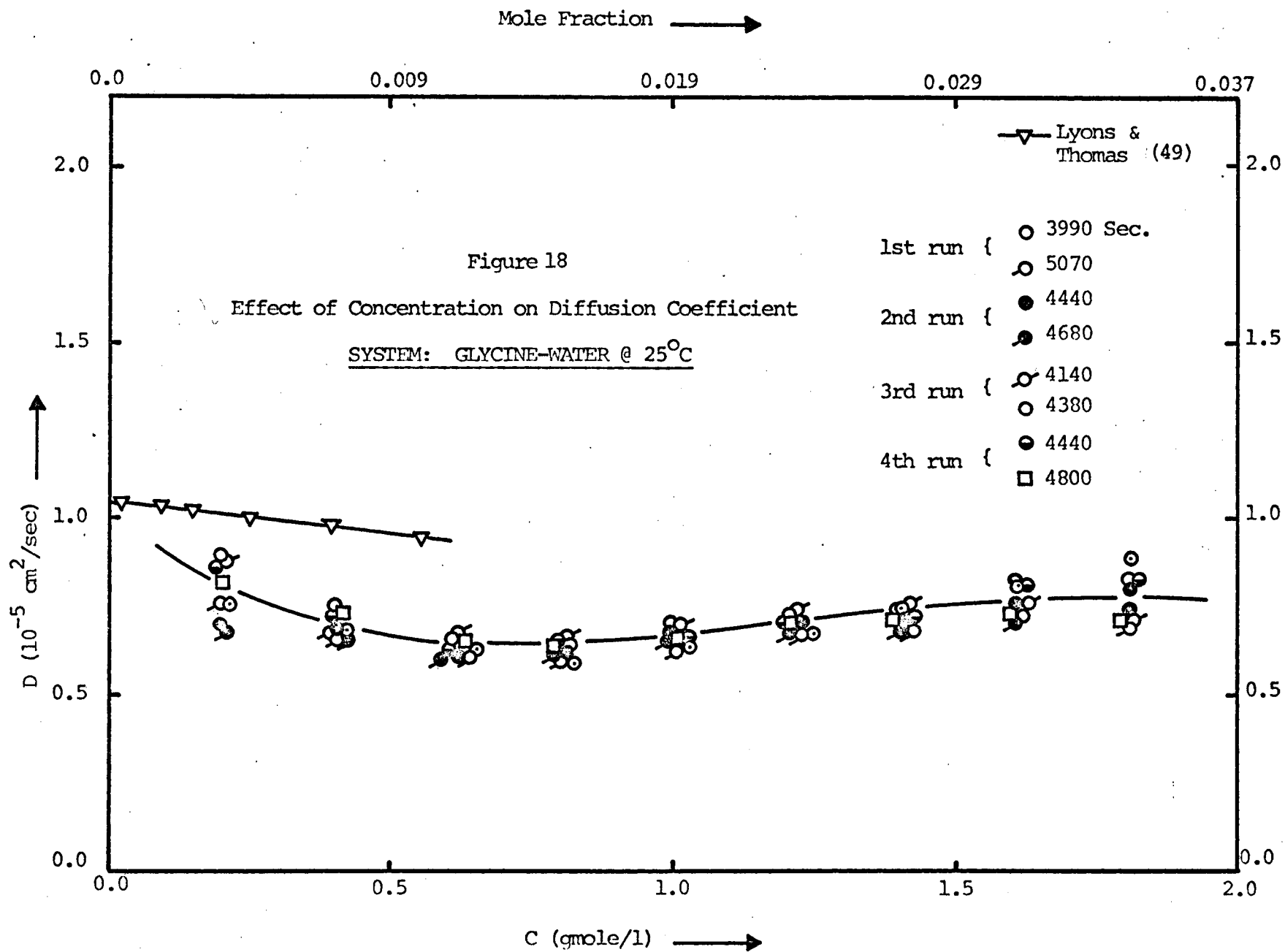
A MIMIC program (44) was used with the finite difference form of the above equation:

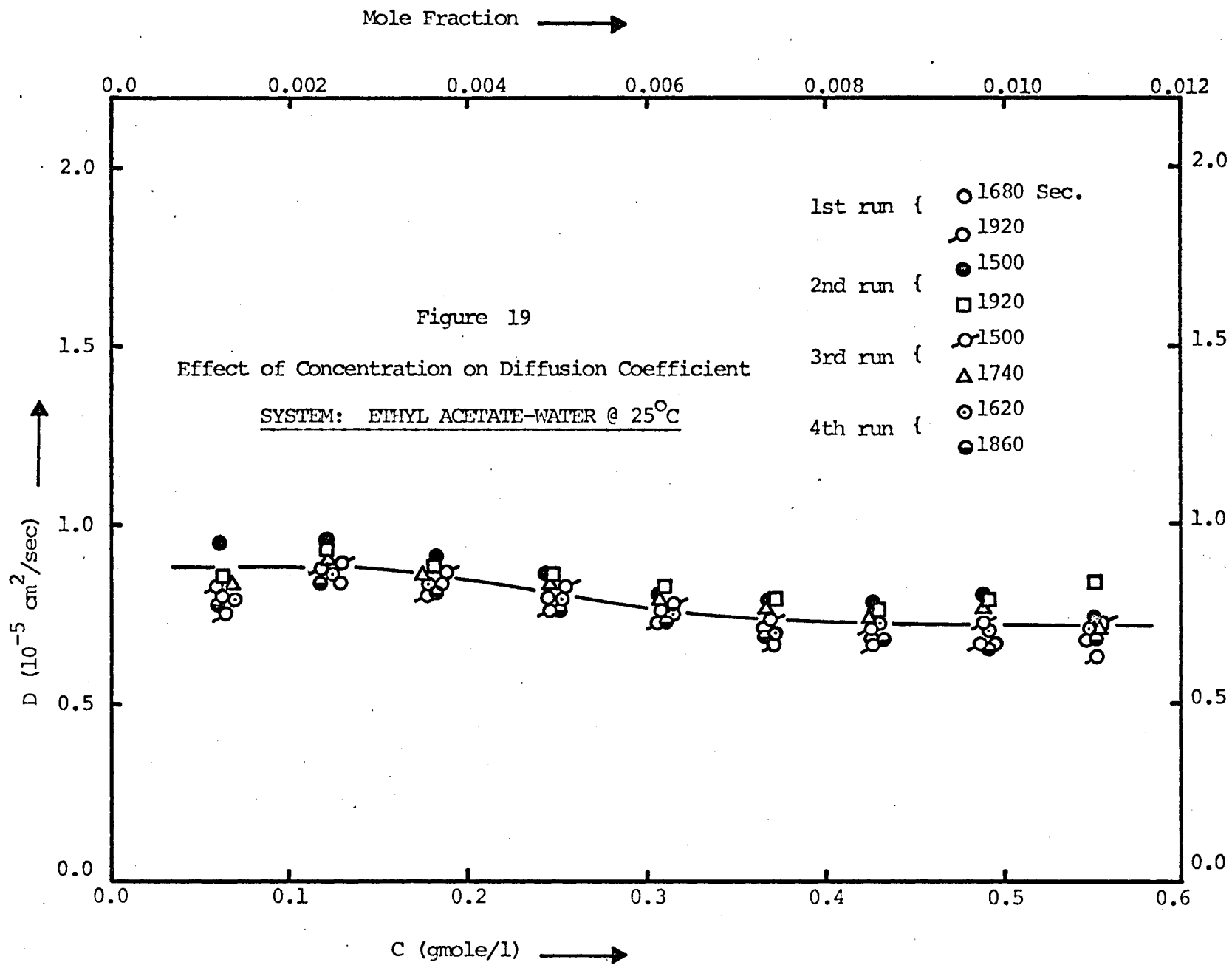
$$\begin{aligned} \frac{\partial c}{\partial t} &= \frac{\partial D}{\partial x} \frac{\partial c}{\partial x} + \frac{\partial^2 c}{\partial x^2} D(c) \\ &= \left[\frac{c_{i+1} - c_{i-1}}{2\Delta x} \right]^2 \frac{dD}{dc} + \left[\frac{c_{i+1} - 2c_i + c_{i-1}}{\Delta x^2} \right] D(c) \end{aligned}$$

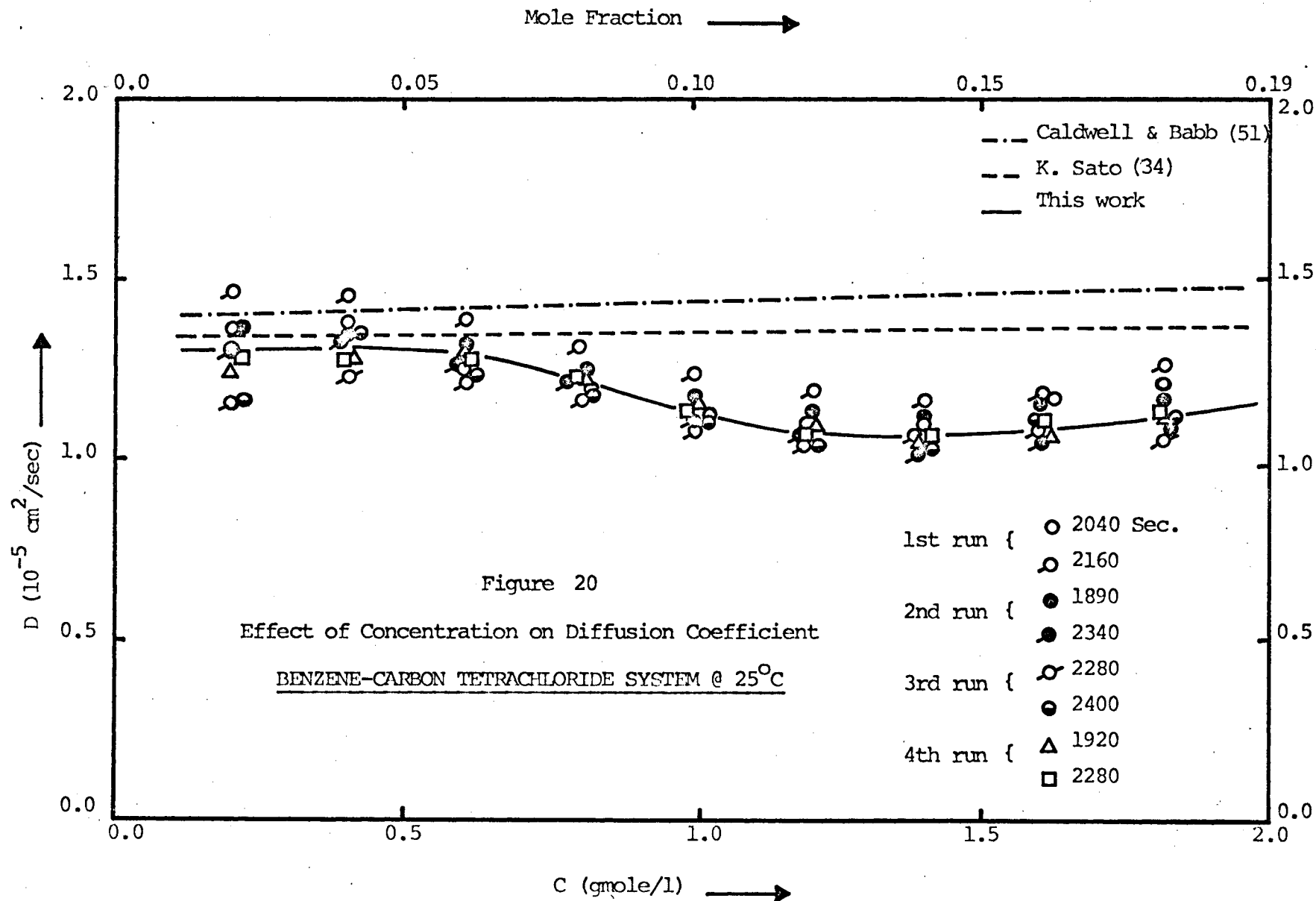
The effective length of the cell (3.0 cm) was divided into 16 sections of 0.1875 cm each. Fifteen integrators were used in the MIMIC program. Results are shown on Figures 21, 22, 23, 24 and 25.











6. DISCUSSION

At first glance, the results obtained agreed reasonably with data found by other researchers. As for the reproducibility of the technique, a survey of diffusion coefficients measured for each system showed that the deviation among results of one system ranged from 3 to 10 percent, seldom over 10 percent. It was also noticed that the deviations are highest at the two extremes of the diffusion coefficient concentration curves. This was due to the fact that the values of u are very small at the ends of the moiré curve, thus when $\frac{l}{u}$ is used in the calculation of D_{AB} , a small deviation of u from the correct value can lead to a highly inaccurate D_{AB} .

It was observed that however tightly the Teflon block was pressed upon the steel body, there always existed a layer of liquid on the top of the lower solution due to leaking from the upper compartment to the lower one when the solutions were not brought into contact with each other. On the other hand, when the Teflon block was pushed to bring the test sections together, convection, however slight, occurred between the 2 phases. Although compared with the whole process of diffusion these effects are not important, they contribute nonetheless to the overall error of the experiment.

As for the time origin, it was taken as the moment when half of the upper test section overlapped the lower one. Since the whole process of pushing the Teflon block to its proper position (when 2 sections are aligned) took only about half a minute, compared with the time when photographs were taken (generally 40, 50 up to 200 minutes after the timer

was started), this way of taking the time origin cannot affect the results significantly. There is, however, a method of correcting the time origin: if the distance x from the boundary is plotted against \sqrt{t} for each concentration of a system, we would obtain a series of straight lines passing through the origin of the $\sqrt{t} - x$ coordinate system if the time origin is correct, assuming that the Boltzmann assumption is valid ($c = f(x/\sqrt{t})$) (39). By trial and error, we can easily determine the correct time origin. Another way of checking the Boltzmann relation is to plot the concentration as a function of x/\sqrt{t} . If the assumption is valid, all points should lie on the same curve.

A major source of error is perhaps due to the tracing of moiré curves from films through the microfilm reader. Since the lines of the graduated screens we used are not thin enough (100 lines per inch), when the film was magnified 10 times by the microfilm reader, the thickness of moiré curves was about 5 mm. Moreover, with the camera used in this project (an Ashahi Pentax model S-1), despite many trials by varying the camera settings, we were not able to get photographs with desired contrast. The moiré curves thus obtained were not as distinct as they should be, especially in the region adjacent to the boundary on the side of the more concentrated solution. With these difficulties we were pleased to measure diffusivities with a deviation of less than 10 percent. It is believed that the temperature control was sufficiently good hence errors caused by fluctuations in temperature were negligible. However, if the optical system is refined an improved temperature control is also recommended.

Before the experiments, solutions interdiffusing were held in a temperature controlled bath for 2 to 3 hours. During the diffusion process

itself, the temperature was again under control. Its fluctuations, if any, were less than 0.1°C .

All main sources of error having been discussed; each system investigated may be worth special considerations now.

6.1 Sucrose - Water System

For this system, the two solutions to diffuse were distilled water and a solution of 0.5N in sucrose. A solution of 1.0N was tried before but since the moiré curves were too high (due to large change in concentration), no results were obtained. This, however, is not a disadvantage of the method. Indeed, experiments can be done with successive concentration ranges provided that the heights of moiré curves do not exceed the width of the test sections and that the linear relation between refractive index and concentration holds up to the concentrations involved. For example, to find diffusivities of the water - sucrose system from zero concentration to 2.0N, we can do experiments with 0.0 - 0.5N, 0.5N - 1.0N, 1.0N - 1.5N and 1.5N - 2.0N solutions.

Data of the sucrose - water system were plotted in Fig. 16 to compare with results found by Sato⁽³⁴⁾ and Irani and Adamson⁽⁴⁵⁾. It can be seen that a fairly good agreement was obtained.

6.2 Sodium Chloride - Water System

The sodium chloride solution used here to diffuse into distilled water is of 2.0N concentration. Diffusion coefficients found for this system were shown in Fig. 17 to compare with results obtained by Stokes⁽⁴⁶⁾ and Sato⁽³⁴⁾ whose experiments were also done at 25°C . A rather good agreement can be seen.

An extrapolation of the diffusion coefficient - concentration

curve gave diffusivity at infinite dilution of $1.08 \times 10^{-5} \text{ cm}^2/\text{sec}$ compared with the value of $1.61 \times 10^{-5} \text{ cm}^2/\text{sec}$ predicted by the Nernst equation⁽²¹⁾. A calculation based on Nernst's equation was presented in the Appendix II.

Diffusivities at concentrations other than zero can be determined by Gordon's relation⁽²²⁾ or the general expression given by Harned⁽⁴⁷⁾. Both relations embodied the principle that the diffusion coefficient is proportional to the gradient of chemical potential. Due to the lack of thermodynamic data, no calculated diffusivity as a function of concentration was available in this report.

It was observed⁽⁴⁾ that the diffusion of ions in electrolyte solutions is dependent not only upon the concentration gradient but also upon the maintenance of electroneutrality in the system. Ions of a diffusing electrolyte may have very different mobilities but every species migrate at the same rate since the interionic forces of attraction accelerate the slower-moving and retard the fast-moving ones. In the presence of other electrolytes, the mobilities of diffusing ions will not be the same as when they are not disturbed. It was also found⁽⁴⁸⁾ that the diffusion of electrolytes may even be influenced by the presence of non-electrolytes. Thus, care must be taken to assure that the presence of other substances in an electrolyte diffusion medium is kept at a minimum level.

6.3 Glycine - Water System

Diffusivities of this system were shown in Fig. 18 in comparison with data obtained by Lyons and Thomas⁽⁴⁹⁾. Unfortunately, the concentration range covered by these researchers was relatively narrow and a comparison of diffusivities at concentrations higher than 0.6N was thus impossible. Nevertheless, it can be seen from Fig. 18 that the compared values differ as much as 25 percent. Lyons and Thomas claimed that

diffusivities given by their experiments, based on the Gouy interference method(24) have a deviation of less than 0.1 percent. On the other hand, results of this work also appeared rather consistent. Moreover, in Lyons & Thomas experiments, the boundary between the two phases was sharpened by sucking out some liquid at the boundary. This might cause some disturbance in the diffusing system and hence the observe diffusivities are somewhat higher than our results.

From the definition of the diffusion coefficients, it can be stated that at infinite dilution, the self-diffusion coefficient is identical to the mutual diffusion coefficient. Thus, it is interesting to note that an extrapolation of the diffusion coefficient-concentration curves reported by Lyons & Thomas, this work and Wang's self diffusion experiments on the glycine - water system⁽⁵⁰⁾ leads almost to the same value of the diffusion coefficient at infinite dilution ($0.95 \times 10^{-5} \text{ cm}^2/\text{sec}$).

6.4 Ethyl Acetate - Water System

The two solutions used here were distilled water and a solution of 0.608N in ethyl acetate which is about the most concentrated solution in ethyl acetate possible at 25°C. Beyond this concentration, there will be phase separation.

Diffusivities found for this system were shown in Fig. 19. Since no data of this system were available in the literature, the diffusion coefficient at infinite dilution obtained by extrapolation of the diffusivity - coefficient curve was used to compare with values predicted by some existing correlations.

According to Fig. 19, the diffusion coefficient at zero ethyl acetate concentration is $0.75 \times 10^{-5} \text{ cm}^2/\text{sec}$ while the Othmer-Thakar correlation⁽²⁰⁾ gave a value of $0.97 \times 10^{-5} \text{ cm}^2/\text{sec}$ and Wilke and Chang's correlation⁽¹⁹⁾ gave $1.04 \times 10^{-5} \text{ cm}^2/\text{sec}$. Sample calculations with these correlations were presented in the Appendix II.

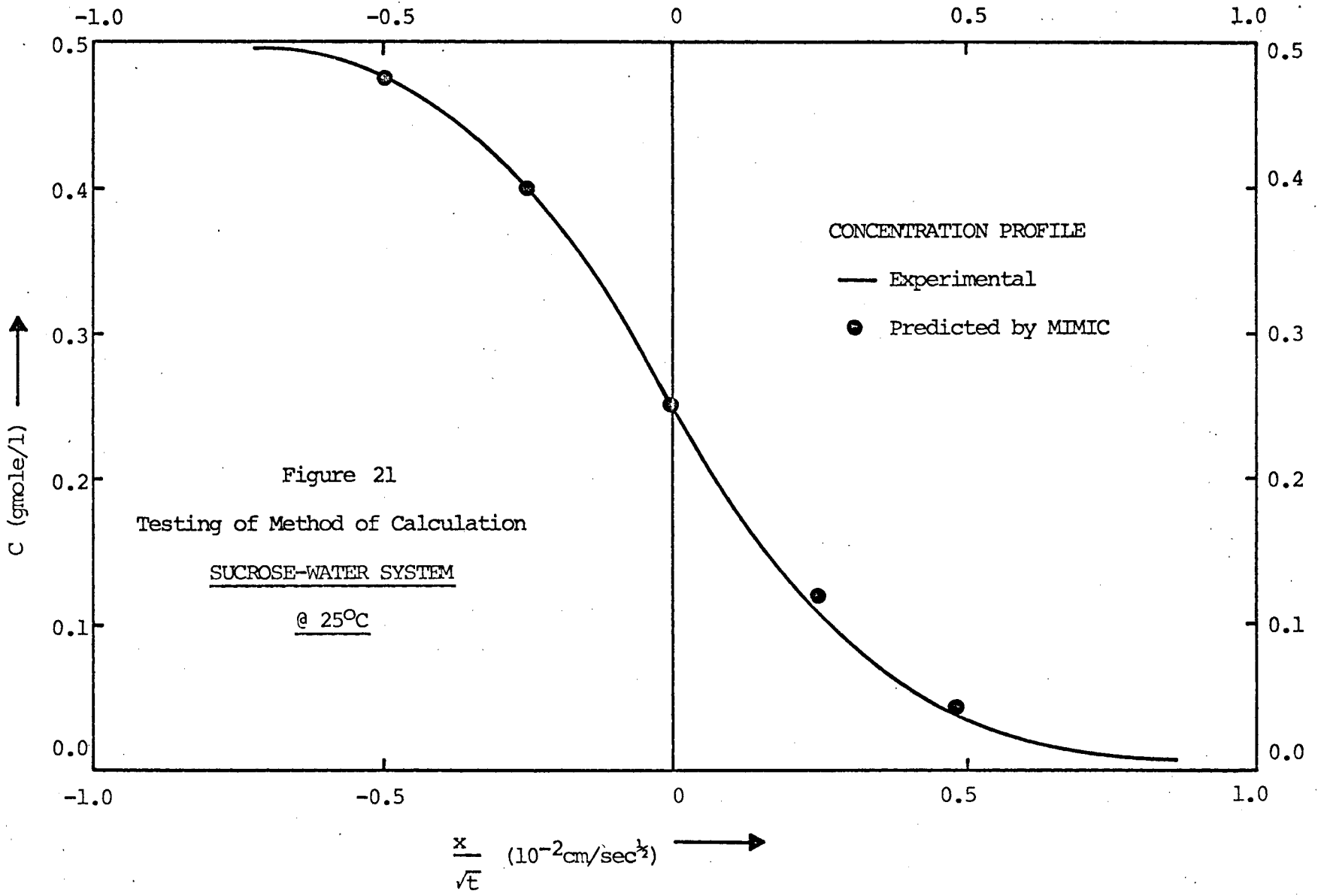
6.5 Benzene - Carbon Tetrachloride System

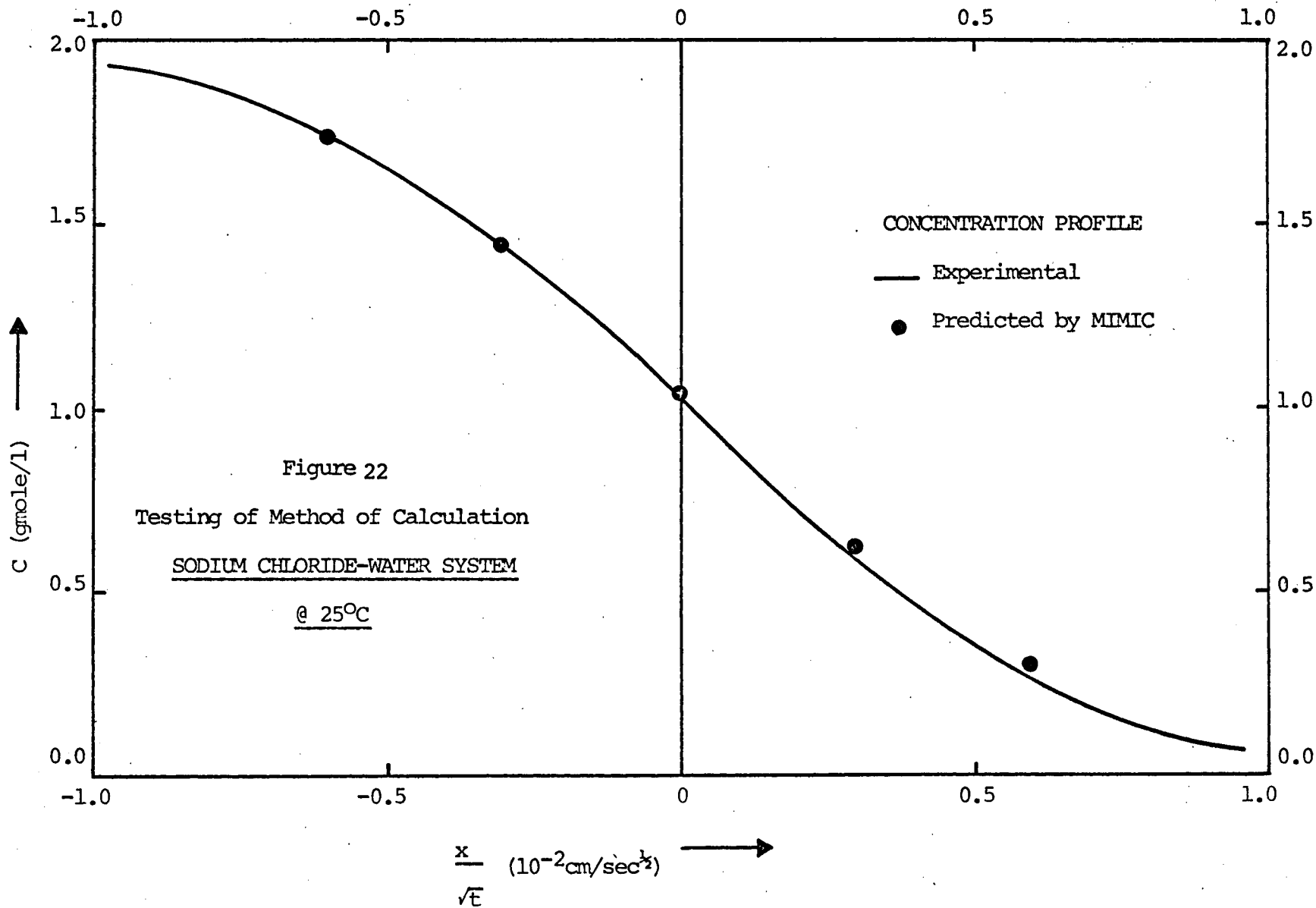
For this system, a solution of 2.012N in benzene was allowed to diffuse into pure carbon tetrachloride. Results were shown in Fig. 20. It can be seen that except in low concentration range, the agreement between these data and those obtained by Caldwell and Babb⁽⁵¹⁾ and Sato et al.⁽³⁴⁾ is not very good: our results are about 15% lower than the findings of these investigators.

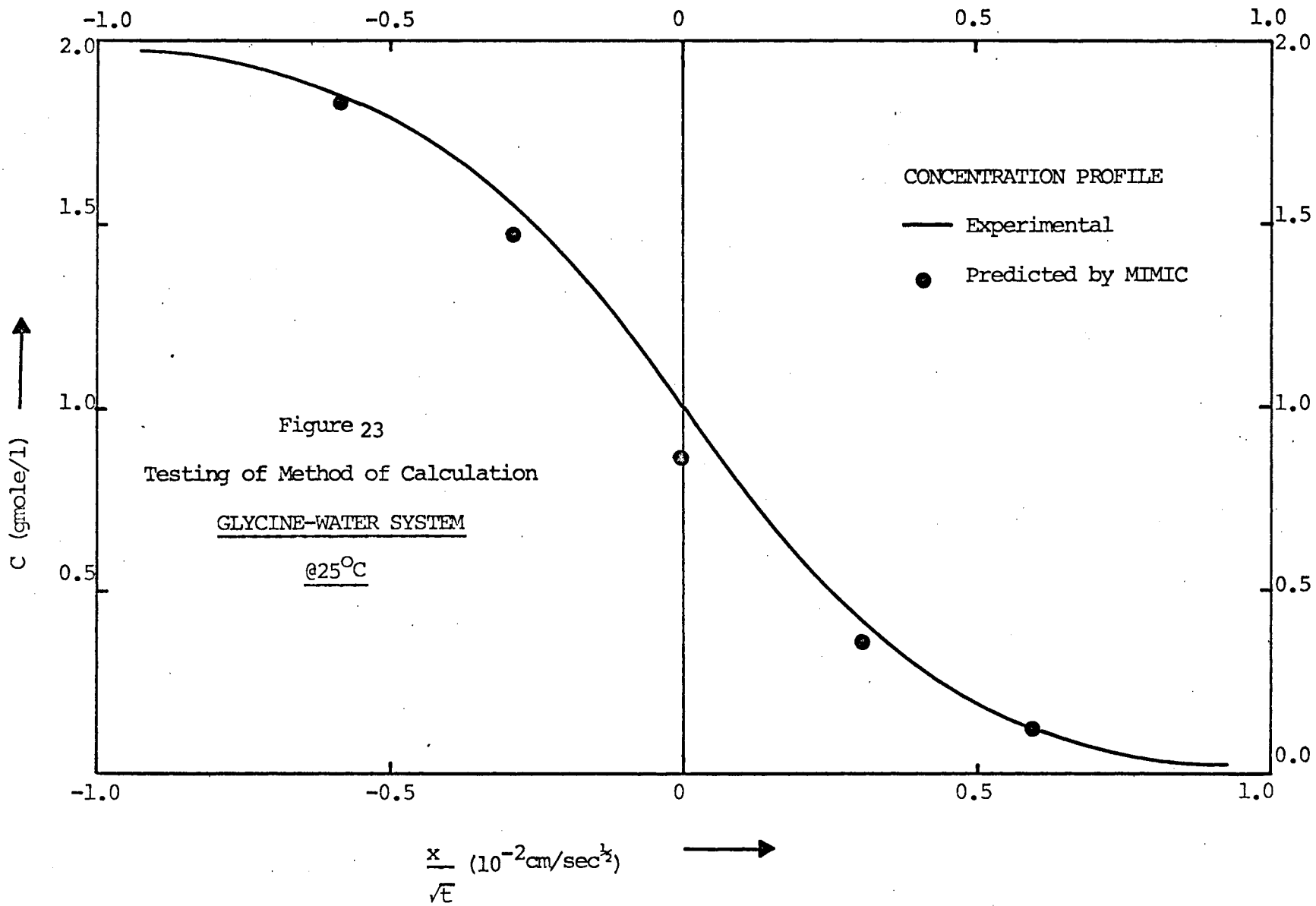
In the case of Sato's data, not only in this system but all the diffusivities found in this project are lower than his. This is perhaps because in his experiments, the lower solution was pushed into the cell under the other one, the region between the two phases was thus submitted to convection before the diffusion process itself.

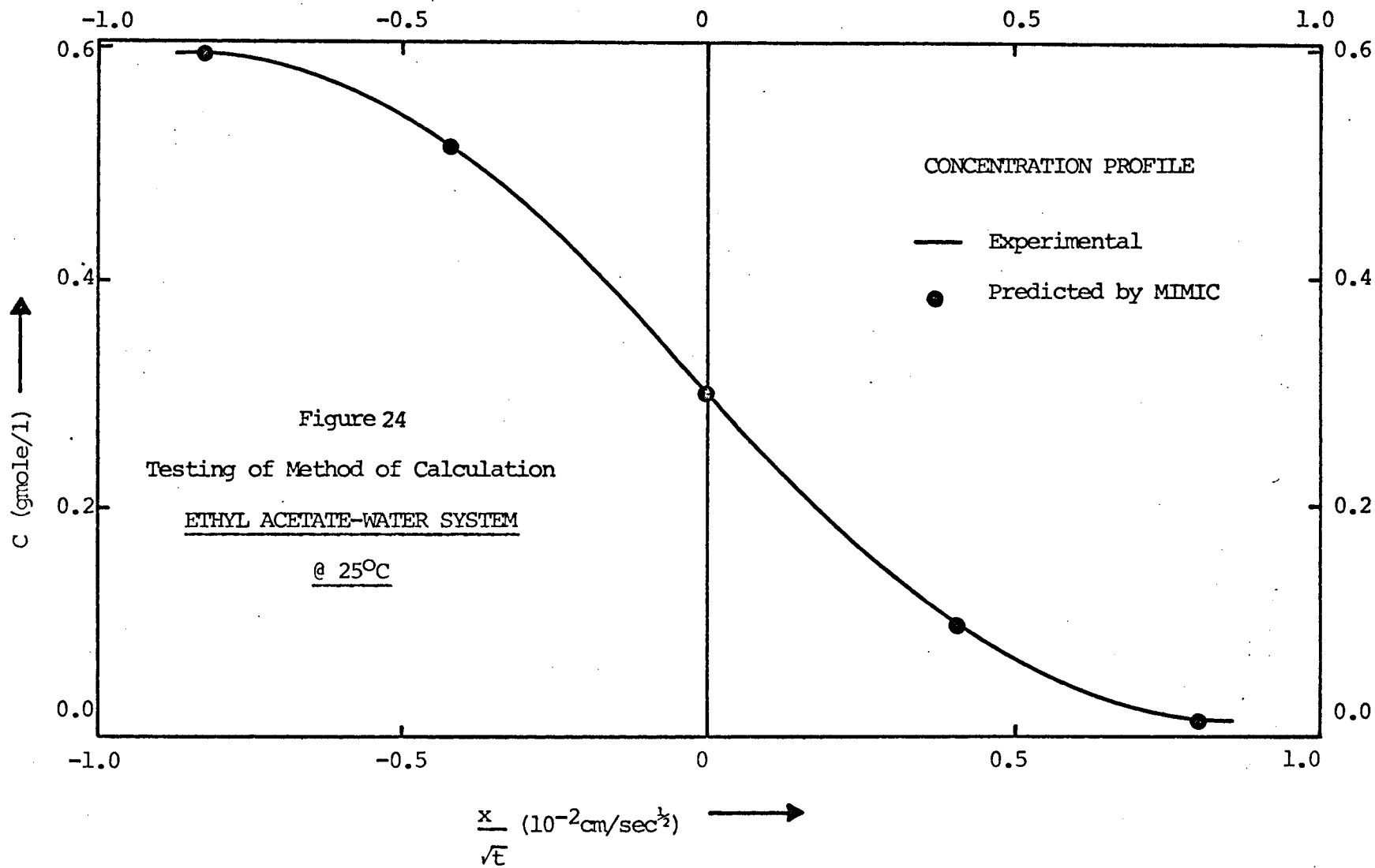
Caldwell and Babb used a single-channel diffusion cell with a Mach-Zehnder interferometer technique. They applied a boundary sharpening method by siphoning out some of the liquid between the 2 diffusing solutions. This might also produce convection as in Sato's case.

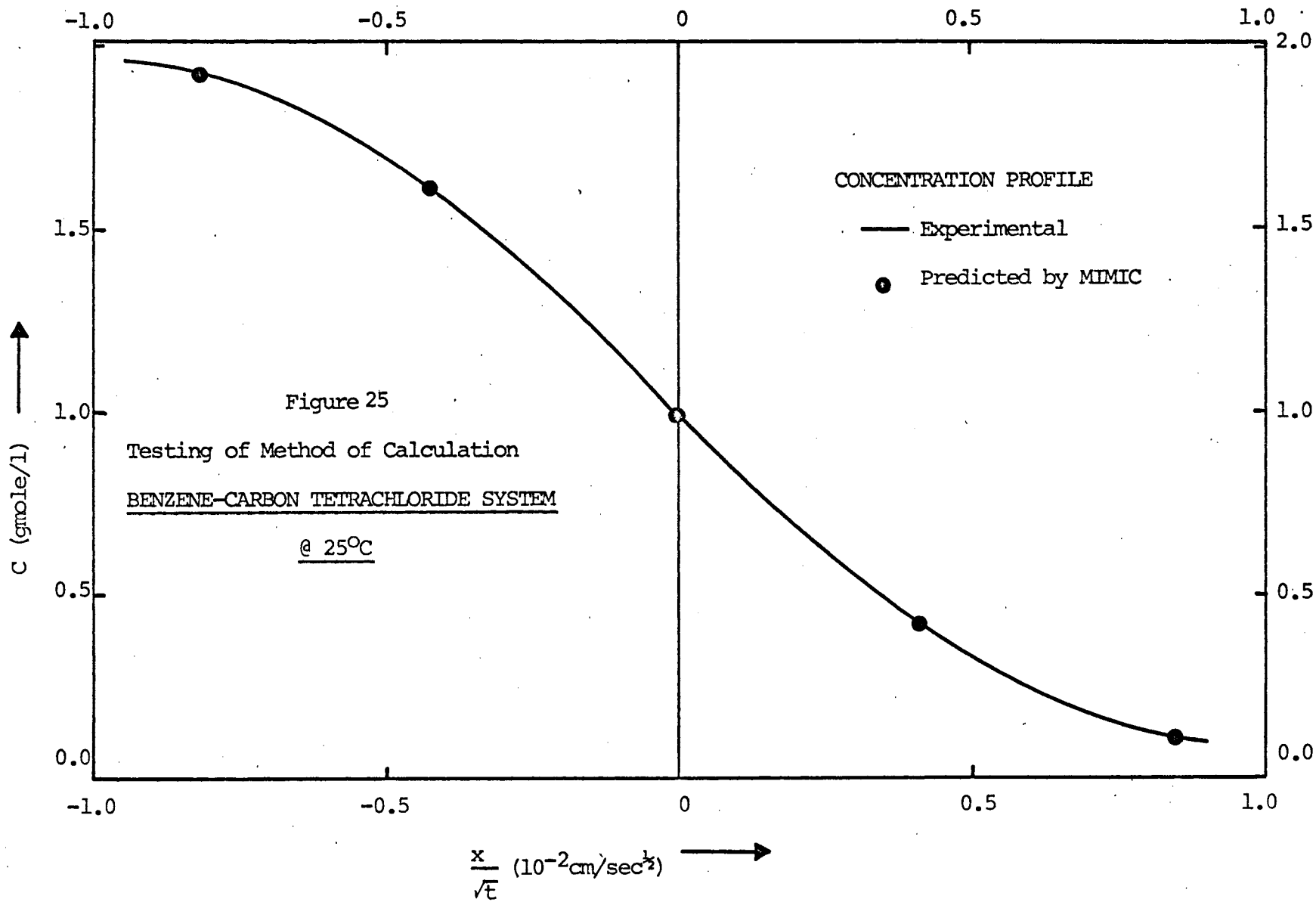
Calculations with the Wilke and Chang correlation gave a diffusivity at infinite dilution of $1.55 \times 10^{-5} \text{ cm}^2/\text{sec}$. An extrapolation of the curve in Fig. 20 yielded $1.21 \times 10^{-5} \text{ cm}^2/\text{sec}$ for infinite dilution.











6.6 Concentration profiles predicted by MIMIC

Figures 21, 22, 23, 24 and 25 show that the experimental concentration profiles are very consistent with the profiles predicted by MIMIC from the experimentally obtained expressions of diffusion coefficient as function of concentration. Thus, we are confident that the method of calculation used here is correct.

6.7 Shape of D vs c curves

Looking back over the results presented here, we will find that the curves of D_{AB} vs c_A generally exhibit a minimum. This is a characteristic of non-ideal solutions. Although we cannot predict at what concentration the diffusion will be maximum or minimum, we are at least able to explain why such a minimum or maximum is possible.

It has been widely agreed that no matter how the expression of the diffusivity is derived, be it from Eyring's kinetic theory, hydrodynamic approach or thermodynamic standpoint, we always have: (52)

$$D_{AB} = \xi \left(1 + \frac{\partial \ln \gamma_A}{\partial \ln x_A} \right) / \mu \quad (6.1)$$

Where ξ is a function of molecular size, intermolecular forces, shape of the molecule and temperature. The second term is a thermodynamic term, indicated the departure of the solution from ideality:

$$1 + \frac{\partial \ln \gamma_A}{\partial \ln x_A} = 1 + \frac{\partial \ln \gamma_B}{\partial \ln x_B} \quad (6.2)$$

γ_A, γ_B : activity coefficients of A, B

μ is the viscosity of the solution.

Thus, we can see from (6.1) that the way diffusivities vary depends on how the last two terms change with concentration.

It is interesting to note here that although the concentration ranges covered in this project are not very large, the diffusivities at infinite dilution found by extrapolation are rather consistent with data from other sources. These diffusivities can be used to deduce diffusivities in concentrated solutions.

One of the simplest correlations has been derived from equation (6.1):

$$\frac{D_{AB}}{D_{AB}^0} = \left(1 + \frac{\partial \ln \gamma_A}{\partial \ln x_A}\right) \frac{\mu_0}{\mu} \quad (6.3)$$

where D_{AB}^0 is the diffusion coefficient at infinite dilution and μ_0 is the viscosity of the solvent.

It can be seen here that D_{AB} is calculable at any concentration provided that D_{AB}^0 as well as viscosity and thermodynamic data of the system are available.

Recently, Vignes⁽⁵³⁾ studied diffusion data of 30 solid and liquid systems and deduced the following correlation:

$$D_{AB} = (D_{AB}^0)^{x_B} (D_{BA}^0)^{x_A} \left(1 + \frac{\partial \ln \gamma_A}{\partial \ln x_A}\right) \quad (6.4)$$

It appeared from his results that his correlation is very accurate and the curves of $\log \left(\frac{D_{AB}}{D_{AB}^0} \left(1 + \frac{\partial \ln \gamma_A}{\partial \ln x_A}\right) \right)$ vs. x_A were all linear.

When the two diffusing species are very similar, $D_{AB}^0 = D_{BA}^0$ and (6.4) simplifies to (6.3), except for the term μ_0/μ . Thus it might be reasonable to add the viscosities into (6.4) as following:

$$D_{AB} = \frac{(D_{AB}^0 \mu_B)^{x_B} (D_{BA}^0 \mu_A)^{x_A}}{\mu} \left(1 + \frac{\partial \ln \gamma_A}{\partial \ln x_A} \right) \quad (6.5)$$

7. CONCLUSIONS AND RECOMMENDATIONS

After analyzing the diffusivities found for 5 inorganic and organic systems, several interesting conclusions have been drawn:

- a. It has been proved that this method offers a quick, simple, efficient way of measuring diffusivities of liquid systems.
- b. The results obtained from this moiré pattern technique are rather crude, with a deviation of about ± 10 percent.
- c. The diffusivities at infinite dilution turned out to be very consistent with many other sources. Whenever thermodynamic data are available, these diffusivities can be used to check values at higher concentrations.
- d. Wider concentration ranges should be covered in order to establish the dependence of diffusivity on concentration from zero to 1.0 mole fraction, to test correlations like (6.3), (6.4) or (6.5) to find the best one.

To improve the accuracy of this technique, some changes in apparatus and technique should be carried out:

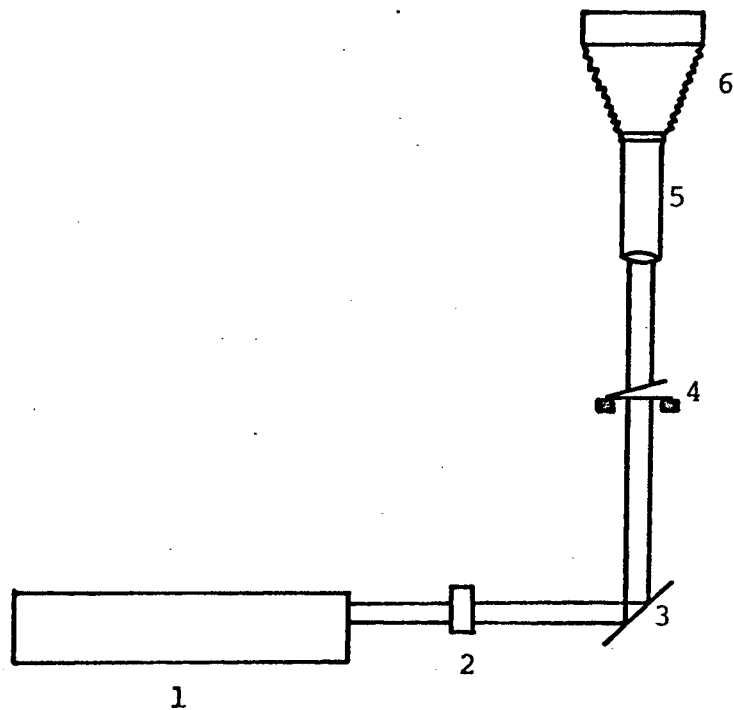
Firstly, since the major source of error comes from the tracing of moiré lines through a microfilm reader, this tracing should be avoided by using the photographs directly. However, such photographs must be clear, have good contrast, and the lines must be thin enough to reduce errors. In order to have all these, a high quality camera should be used along with more finely graduated screens. It is suggested that a Hasselblad 500C is good enough. On the other hand, screens of about 1000 lines per inch are recommended. Of course, with these cameras and screens, a new light source, brighter than the presently used (a K25 Sylvania concentrated arc lamp) would be necessary. Whenever possible, an interference filter would be desirable to produce highly monochromatic light. The optical system could be further improved by using a finer ground glass and a higher quality lens to produce parallel light beam.

As far as the diffusion cell is concerned, the present cell is reasonably good but when it is expected to be in use for a long time, the Teflon block should be replaced by one made of Delrin (suggested by Mr. L.J. Suggett of the Faculty of Engineering Machine Shop, McMaster University) since it does not subject to shrinking as much as Teflon.

If the liquids interdiffusing are not very volatile, an alternative technique can be used to measure diffusivities more quickly and perhaps, more accurately than the moiré pattern method. This technique, called the microinterferometric method, has been used by Nishijima and Oster⁽³¹⁾, Secor⁽³²⁾ and recently by Paul⁽⁵⁴⁾ to measure diffusion coefficients for concentrated solutions, including some polymer systems. Details of this method can be found in the above references.

To have a higher accuracy, it is suggested that: 1. a laser beam be used instead of the combination of a point source and a collimator lens; 2. the temperatures of solutions interdiffusing should be controlled by containing them in two constant temperature syringes placed besides the diffusion cell; 3. the concentration profile be fitted to a sigmoid equation (S-shaped curve) to avoid calculation errors due to integration and differentiation.

A setup recommended for this method is shown in Fig. 26.



1: gas laser; 2: water filter; 3: mirror
4: diffusion cell; 5: microscope; 6: camera

Figure 26

Diffusion Measurement by Laser Interference

8. NOMENCLATURE

- a - thickness of the diffusion cell
- b - distance from the diffusion cell to the screen where deflections of the light beam were measured
- c - concentration
- D - diffusion coefficient
- \hat{D} - intrinsic diffusion coefficient, defined by (3.1.11) and (3.1.12)
- g - function defined by (3.1.19)
- k - constant in equation (3.2.15)
- K - constant in equation (3.2.17)
- n - refractive index
- N - molar flux in the x-direction
- s - area under the curve of u vs x from $x = 0$ to $x = x$ (Fig. 5a)
- S - total area under the curve of u vs x
- t - diffusion time
- u - height of moiré curve
- v - velocity of the bulk flow
- \bar{V} - partial molal volume
- x - distance from the boundary, in the direction of diffusion
- x - (subscripted) molar fraction
- y - distance in the direction perpendicular to the direction of diffusion
- z - deflection of the light beam when emerging from the diffusion cell

Greek Symbols

- γ - activity coefficient
 μ - viscosity
 η - Boltzmann variable
 ρ - radius of curvature of the deviated light beam
 ψ - angle defined in Fig. 1
 θ_1 - - ibid -
 θ_2 - - ibid -
 ϕ - angle between the lines of the two screens (A) and (D) in Fig. 2b
 ξ - constant in equation (6.1)

Subscripts

- A - refers to one of the two diffusing species
B - - ibid -
1 - refers to the solvent or the solution of lower concentration
o - refers to the solution of higher concentration
AB - refers to the diffusion of species A into species B
BA - refers to the diffusion of species B into species A
 $\frac{o}{AB}$ - $\frac{o}{BA}$ - refers to the diffusion coefficient at infinite dilution

9. REFERENCES

- *1. Einstein, A. : Ann. Physik, 17 (4), 549 (1905)
- *2. Fick, A. : Ann. Physik, 94, 59 (1855)
- *3. Fourier, J.B. : Théorie analytique de la chaleur, Oeuvres de
Fourier (1822)
- 4. Geddes, A.L. and Pontius, R.B. : "Determination of Diffusivity",
Physical Methods, Part II, Technique of Organic
Chemistry, Vol. 1, p.865 (1960, Interscience Pub.)
- *5. Gilliland, E.R. : Ind. Eng. Chem., 26, 681 (1932)
- *6. Hirschfelder, J.O., Bird, R.B. and Spatz, E.L. : Trans. A.S.M.E.,
71, 921 (1949)
- *7. Slattery, J.C. and Bird, R.B. : A.I.Ch.E.J., 4, 137 (1958)
- 8. Bird, R.B., Stewart, W.E. and Lightfoot, E.N. : "Transport Phenomena",
John Wiley & Sons, Inc. New York, London and Sydney
(1965)
- *9. Loschmidt, J. : Wien. Ber. 61, 367 (1870)
- *10. Loschmidt, J. : Wien. Ber. 62, 468 (1870)
- *11. Stefan, J. : Wien. Ber. (II) 68, 385 (1874)
- *12. Stefan, J. : Wien. Ber. (II) 98, 1418 (1889)
- *13. Stefan, J. : Ann. Physik (3) 41, 725 (1890)
- *14. Obermayer, A. von : Wien. Ber. 81 (II), 1102 (1880)
- 15. Arnold, J.H. : J. Am. Chem. Soc. 52, 3937 (1930)
- 16. Eyring, H. et.al. : "The Theory of Rate Processes" McGraw Hill
Book Company, Inc., New York and London (1941)
- 17. Crank, K. and Hartley, G.S. : Trans. Faraday Soc., 45, 801 (1949)

- *18. Lightfoot, E.N. and Cussler, E.L. Jr. : Chem. Eng. Symposium Ser.
58, 61, 66 (1965)
19. Wilke, C.R. and Chang, P. : Am. Inst. Chem. Eng. J. 1, 264 (1955)
20. Othmer, D.F. and Thakar, M.S. : Ind. Eng. Chem., 45, 589 (1953)
- *21. Nernst, Z. : Physik Chem., 2, 613 (1888)
- *22. Gordon : J. Chem. Phys., 5, 522 (1937)
23. Northrop, J.H. and Anson, M.L. : J. Gen. Physiol. 12, 543 (1929)
- *24. Gouy, G.L. : Comp. rend., 90, 307 (1880)
- *25. Wiener, O. : Wied. Ann., 49, 105 (1893)
26. Thovert, J. : Ann. Chim. phys. (7) 26, 366 (1902)
- *27. Kegeles, G. and Gosting, L.J. : J. Am. Chem. Soc., 69, 2516 (1947)
28. Longworth, L.J. : J. Am. Chem. Soc. 69, 2510 (1947)
- *29. Coulson, C.A. et al. : Proc. Roy. Soc. A192, 382 (1948)
30. Robinson, C. : Proc. Roy. Soc. A204, 339 (1950)
31. Nishijima, Y. and Oster, G. : J. Chem. Education, 38, 114 (1961)
32. Secor, R.M. : A.I.Ch.E.J., (3) 11, 442 (1965)
- *33. Lamm, O. : Z. Physik Chem. A138, 313 (1928)
34. Sato et al. : Kagaku Kōgaku, 28, 445 (1964)
35. Boltzmann, L. : Ann. Physik, Leipzig, 53 959 (1894)
36. Prager, S. : J. Chem. Phys., 21, 1344 (1953)
37. Takamatsu, T. et al. : Kagaku Kōgaku, 28, 755 (1964)
- *38. Stefan, J. : Wiener Bet., (II) 78, 987 (1878)
39. Münter, E. : Ann. Phys., 11, 558 (1931)
40. Lamm, O. : Nova Acta Reg. Soc. Scient. upsaliensis Ser. IV, 10,
Nr. 6 (1937)

41. Jost, W. : "Diffusion in Solid, Liquid, Gases" Academic Press,
New York (1952)
- *42. Sato, K. and Miyamoto, K. : Reprint of the Annual Meeting of the
Soc. Chem. Engrs., Japan, April 1959, p.93
43. Oster, G. and Nishijima, Y. : "Moiré Patterns", Scientific
American, 54 (May 1963)
44. Northcott, T.H. : M.Eng. Thesis, Department of Chemical Engineering
McMaster University, October 1967
45. Irani, R.R. and Adamson, A.V. : J. Phys. Chem., 62, 1517 (1958)
46. Stokes, R.H. : J. Am. Chem. Soc., 72, 2243 (1950)
- *47. Harned, H.S. : Natl. Bur. Standards (U.S.) Cir. No. 524, 69 (1953)
- *48. McBain, J.W. and Liu, T.H. : J. Am. Chem. Soc., 53, 59 (1931)
49. Lyons, M.S. and Thomas, J.V. : J. Am. Chem. Soc., 72, 4506 (1950)
50. Wang, J.H. : J. Am. Chem. Soc., 75, 2777 (1953)
51. Caldwell, C.S. and Babb, A.L. : J. Phys. Chem., 60, 51 (1956)
52. Johnson, P.A. and Babb, A.L. : Chem. Rev., 56, 387 (1956)
53. Vignes, A. : Ind. Eng. Chem., (2) 5, 189 (1966)
54. Paul, D.R. : I & E C Fundamentals, (2) 6, 217 (1967)
55. Crank, J. : "The Mathematics of Diffusion"., Oxford at the
Clarendon Press, London (1967), P. 225.
56. Robinson and Stokes : "Electrolyte Solutions", Butterworth,
London (1955), P. 452

* These references were not read in original form.

APPENDICES

Appendix IDerivation of the Expression for Diffusivities when there is Volume Change on Mixing

The diffusion equations for this case are:

$$N_A = -D_A \frac{\partial C_A}{\partial x} + x_A (N_A + N_B) \quad (\text{A.1.1})$$

$$N_B = -D_B \frac{\partial C_B}{\partial x} + x_B (N_A + N_B) \quad (\text{A.1.2})$$

Where D_A and D_B are the intrinsic diffusion coefficients (55) of A and B.

If v is the velocity of the bulk flow, assumed to be in the x -direction and to depend on x and t only, we have:

$$N_A = -D_A \frac{\partial C_A}{\partial x} + vC_A \quad (\text{A.1.3})$$

$$N_B = -D_B \frac{\partial C_B}{\partial x} + vC_B \quad (\text{A.1.4})$$

Now if \bar{V}_A and \bar{V}_B are the partial molal volumes of A and B, since in 1 unit of overall volume we have $\bar{V}_A C_A$ volume unit of A and $\bar{V}_B C_B$ volume unit of B,

$$\bar{V}_A C_A + \bar{V}_B C_B = 1 \quad (\text{A.1.5})$$

Which can be differentiated to give, at constant pressure and temperature:

$$\left(\frac{\partial C_B}{\partial C_A} \right)_{P,T} = - \frac{\bar{V}_A}{\bar{V}_B} \quad (\text{A.1.6})$$

On the other hand, a material balance gives us:

$$\frac{\partial N_A}{\partial x} = - \frac{\partial C_A}{\partial t} \quad (\text{A.1.7})$$

$$\frac{\partial N_B}{\partial x} = - \frac{\partial C_B}{\partial t} \quad (\text{A.1.8})$$

Equations (A.1.1) and (A.1.2) become:

$$\frac{\partial C_A}{\partial t} = \frac{\partial}{\partial x} \left(D_A \frac{\partial C_A}{\partial x} \right) - \frac{\partial}{\partial x} (v C_A) \quad (\text{A.1.9})$$

$$\frac{\partial C_B}{\partial t} = \frac{\partial}{\partial x} \left(D_B \frac{\partial C_B}{\partial x} \right) - \frac{\partial}{\partial x} (v C_B) \quad (\text{A.1.10})$$

Inserting (A.1.5) and (A.1.6) in (A.1.10), we get:

$$- \frac{\bar{V}_A}{\bar{V}_B} \frac{\partial C_A}{\partial t} = - \frac{\partial}{\partial x} \left(D_B \frac{\bar{V}_A}{\bar{V}_B} \frac{\partial C_A}{\partial x} \right) - C_B \frac{\partial v}{\partial x} - v \frac{\partial C_B}{\partial x} \quad (\text{A.1.11})$$

This, when added to (A.1.10) multiplied by $\frac{\bar{V}_A}{\bar{V}_B}$ gives:

$$\begin{aligned} 0 = & - \frac{\partial}{\partial x} \left(D_B \frac{\bar{V}_A}{\bar{V}_B} \frac{\partial C_A}{\partial x} \right) - C_B \frac{\partial v}{\partial x} + v \frac{\bar{V}_A}{\bar{V}_B} \frac{\partial C_A}{\partial x} \\ & + \frac{\bar{V}_A}{\bar{V}_B} \frac{\partial}{\partial x} \left(D_A \frac{\partial C_A}{\partial x} \right) - C_A \frac{\bar{V}_A}{\bar{V}_B} \frac{\partial v}{\partial x} - v \frac{\bar{V}_A}{\bar{V}_B} \frac{\partial C_A}{\partial x} \end{aligned}$$

or, after a simplification:

$$(C_A \bar{V}_B + C_B \bar{V}_A) \frac{\partial v}{\partial x} = - \bar{V}_B \frac{\partial}{\partial x} \left(D_B \frac{\bar{V}_A}{\bar{V}_B} \frac{\partial C_A}{\partial x} \right) + \bar{V}_A \frac{\partial}{\partial x} \left(D_A \frac{\partial C_A}{\partial x} \right) \quad (\text{A.1.12})$$

Since $C_A \bar{V}_A + C_B \bar{V}_B = 1$,

$$\frac{\partial v}{\partial x} = \bar{V}_A \frac{\partial}{\partial x} \left(D_A \frac{\partial C_A}{\partial x} \right) - \bar{V}_B \frac{\partial}{\partial x} \left(D_B \frac{\partial \bar{V}_A}{\partial x} \frac{\partial C_A}{\partial x} \right) \quad (\text{A.1.13})$$

After a regrouping of the above relation, we have:

$$\frac{\partial v}{\partial x} = \bar{V}_A \frac{\partial}{\partial x} (D_A - D_B) \frac{\partial C_A}{\partial x} - \bar{V}_B D_B \frac{\partial C_A}{\partial x} \frac{\partial}{\partial x} \left(\frac{\bar{V}_A}{\bar{V}_B} \right) \quad (\text{A.1.14})$$

An integration of (A.1.14) from $x = -\infty$ to $x = x$ gives:

$$\begin{aligned} \int_{x=-\infty}^{x=x} dv &= \underbrace{\int_{-\infty}^x \bar{V}_A \frac{\partial}{\partial x} \left[(D_A - D_B) \frac{\partial C_A}{\partial x} \right] dx}_1 \\ &- \underbrace{\int_{-\infty}^x \bar{V}_B D_B \frac{\partial C_A}{\partial x} \frac{\partial}{\partial x} \left(\frac{\bar{V}_A}{\bar{V}_B} \right) dx}_2 \end{aligned} \quad (\text{A.1.15})$$

Assuming that v and $\frac{\partial C_A}{\partial x}$ are zero at $x = -\infty$, we have:

$$v = 1 + 2$$

where:

$$\begin{aligned} 1 &= \bar{V}_A (D_A - D_B) \frac{\partial C_A}{\partial x} - \int_{-\infty}^x (D_A - D_B) \frac{\partial C_A}{\partial x} \frac{\partial \bar{V}_A}{\partial x} dx \\ 2 &= \int_{-\infty}^x \left(D_B \frac{\partial C_A}{\partial x} \frac{\partial \bar{V}_A}{\partial x} - D_B \frac{\partial C_A}{\partial x} \frac{\bar{V}_A}{\bar{V}_B} \frac{\partial \bar{V}_B}{\partial x} \right) dx \end{aligned}$$

Hence:

$$v = \bar{V}_A (D_A - D_B) \frac{\partial C_A}{\partial x} + \int_{-\infty}^x \left(-D_A \frac{\partial \bar{V}_A}{\partial x} + \frac{\bar{V}_A}{\bar{V}_B} D_B \frac{\partial \bar{V}_B}{\partial x} \right) \frac{\partial C_A}{\partial x} dx \quad (\text{A.1.17})$$

Replacing $\frac{\partial \bar{V}_A}{\partial x}$ by $\frac{\partial \bar{V}_A}{\partial \bar{V}_B} \cdot \frac{\partial \bar{V}_B}{\partial C_A} \cdot \frac{\partial C_A}{\partial x}$ we obtain:

$$v = \bar{V}_A (\mathcal{D}_A - \mathcal{D}_B) \frac{\partial C_A}{\partial x} + \int_{-\infty}^x (-\mathcal{D}_A \frac{\partial \bar{V}_A}{\partial \bar{V}_B} + \frac{\bar{V}_A}{\bar{V}_B} \mathcal{D}_B) \left(\frac{\partial \bar{V}_B}{\partial C_A} \right) \left(\frac{\partial C_A}{\partial x} \right)^2 dx$$

(A.1.18)

Now since $\bar{V}_A C_A + \bar{V}_B C_B = 1$,

$$\frac{\partial \bar{V}_A}{\partial \bar{V}_B} = - \frac{C_B}{C_A}$$

(A.1.18) becomes:

$$v = \bar{V}_A (\mathcal{D}_A - \mathcal{D}_B) \frac{\partial C_A}{\partial x} + \int_{-\infty}^x (\mathcal{D}_A \frac{C_B}{C_A} + \frac{\bar{V}_A}{\bar{V}_B} \mathcal{D}_B) \left(\frac{\partial \bar{V}_B}{\partial C_A} \right) \left(\frac{\partial C_A}{\partial x} \right)^2 dx$$

(A.1.19)

Substituting (A.1.19) to (A.1.9), we get:

$$\begin{aligned} \frac{\partial C_A}{\partial t} = \frac{\partial}{\partial x} \left(\mathcal{D}_A \frac{\partial C_A}{\partial x} \right) - \frac{\partial}{\partial x} \left\{ C_A \left(\bar{V}_A (\mathcal{D}_A - \mathcal{D}_B) \frac{\partial C_A}{\partial x} + \int_{-\infty}^x \frac{C_B}{C_A} \right. \right. \\ \left. \left. (\mathcal{D}_A + \mathcal{D}_B \frac{\bar{V}_A}{\bar{V}_B} \frac{C_A}{C_B}) \left(\frac{\partial \bar{V}_B}{\partial C_A} \right) \left(\frac{\partial C_A}{\partial x} \right)^2 dx \right\} \end{aligned} \quad (A.1.20)$$

Or after a rearrangement:

$$\begin{aligned} \frac{\partial C_A}{\partial t} = \frac{\partial}{\partial x} \left\{ \mathcal{D}_A - C_A \bar{V}_A (\mathcal{D}_A - \mathcal{D}_B) \right\} \frac{\partial C_A}{\partial x} \\ - \frac{\partial}{\partial x} \left\{ C_A \int_{-\infty}^x (\mathcal{D}_A + \mathcal{D}_B \frac{\bar{V}_A}{\bar{V}_B} \frac{C_A}{C_B}) \left(\frac{\partial \bar{V}_B}{\partial C_A} \right) \left(\frac{\partial C_A}{\partial x} \right)^2 dx \right\} \end{aligned} \quad (A.1.21)$$

By defining a new diffusion coefficient D:

$$D = \bar{D}_A \bar{V}_B C_B + \bar{D}_B \bar{V}_A C_A \quad (\text{A.1.22})$$

We have:

$$\begin{aligned} \bar{D}_A - C_A \bar{V}_A (\bar{D}_A - \bar{D}_B) &= \bar{D}_A (1 - C_A \bar{V}_A) + \bar{D}_B C_A \bar{V}_A \\ &= C_B \bar{V}_B \bar{D}_A + C_A \bar{V}_A \bar{D}_B \end{aligned}$$

$$\bar{D}_A - C_A \bar{V}_A (\bar{D}_A - \bar{D}_B) = D \quad (\text{A.1.23})$$

and:

$$\frac{\bar{D}}{\bar{V}_B C_B} = \bar{D}_A + \bar{D}_B \frac{\bar{V}_A C_A}{\bar{V}_B C_B} \quad (\text{A.1.24})$$

Thus (A.1.21) becomes:

$$\frac{\partial C_A}{\partial t} = \frac{\partial}{\partial x} \left(D \frac{\partial C_A}{\partial x} \right) - \frac{\partial}{\partial x} \left\{ C_A \int_{-\infty}^x \frac{D}{C_A \bar{V}_B} \left(\frac{\partial \bar{V}_B}{\partial C_A} \right) \left(\frac{\partial C_A}{\partial x} \right)^2 dx \right\} \quad (\text{A.1.25})$$

Similarly,

$$\frac{\partial C_B}{\partial t} = \frac{\partial}{\partial x} \left(D \frac{\partial C_B}{\partial x} \right) - \frac{\partial}{\partial x} \left\{ C_B \int_{-\infty}^x \frac{D}{C_A \bar{V}_B} \left(\frac{\partial \bar{V}_B}{\partial C_A} \right) \left(\frac{\partial C_A}{\partial x} \right)^2 dx \right\} \quad (\text{A.1.26})$$

By defining a function $g(C_A)$ such that:

$$g(C_A) = \frac{1}{C_A \bar{V}_B} \left(\frac{\partial \bar{V}_B}{\partial C_A} \right),$$

the previous relations can be written as follows:

$$\frac{\partial C_A}{\partial t} = \frac{\partial}{\partial x} \left(D \frac{\partial C_A}{\partial x} \right) + \frac{\partial}{\partial x} \left\{ C_A \int_{-\infty}^x D g(C_A) \left(\frac{\partial C_A}{\partial x} \right)^2 dx \right\} \quad (\text{A.1.27})$$

and:

$$\frac{\partial C_B}{\partial t} = \frac{\partial}{\partial x} \left(D \frac{\partial C_B}{\partial x} \right) + \frac{\partial}{\partial x} \left\{ C_B \int_{-\infty}^x D g(C_A) \left(\frac{\partial C_A}{\partial x} \right)^2 dx \right\} \quad (\text{A.1.28})$$

With a Boltzmann variable defined as $\eta = \frac{x}{\sqrt{t}}$ and the following boundary

conditions:

$$C_A = C_0 \text{ at } x < 0, t = 0$$

$$C_A = C_1 \text{ at } x > 0, t = 0$$

equation (A.1.27) can be transformed to:

$$\eta \frac{dC_A}{d\eta} = -2 \frac{d}{d\eta} \left(D \frac{dC_A}{d\eta} \right) - 2 \frac{d}{d\eta} \left\{ C_A \int_{-\infty}^{\eta} D g(C_A) \left(\frac{dC_A}{d\eta} \right)^2 d\eta \right\} \quad (\text{A.1.29})$$

Since $D \frac{dC_A}{d\eta} = \left(D \frac{\partial C_A}{\partial x} \right) \left(\frac{\partial x}{\partial \eta} \right) = \sqrt{t} \left(D \frac{\partial C_A}{\partial x} \right) = 0$ at $x = -\infty$ or

$\eta = -\infty$, we have the following expression for the diffusion coefficient

D , assuming that D of the second term on the right hand side of (A.1.29)

can be approximated by $-\frac{1}{2} \frac{d\eta}{dC_A} \int_{C_0}^{C_A} \eta dC_A$ (case of no volume change on mixing):

$$D \Big|_{C_A = C_A} = -\frac{1}{2} \frac{d\eta}{dC_A} \left\{ \int_{C_0}^{C_A} \eta dC_A - C_A \int_{C_0}^{C_A} g(C_A) \left(\int_{C_0}^{C_A} \eta dC_A \right) dC_A \right\}$$

(A.1.30)

Thus, diffusion coefficients of systems displaying volume change on mixing can be calculated through the same ways as in the case of systems without volume change on mixing, provided that thermodynamic data, i.e. the $g(C_A)$ values are available.

Appendix II

Estimation of Diffusivities at Infinite Dilution

The two most famous correlations used to estimate diffusion coefficients in dilute solutions are the equations of Wilke and Chang⁽¹⁹⁾ and Othmer and Thakar⁽²⁰⁾.

The Wilke-Chang's equation is:

$$D_o = 7.4 \times 10^{-8} \frac{T (XM)^{0.5}}{\mu (V_o)^{0.6}} \quad (\text{A.2.1})$$

where D_o is the diffusion coefficient at infinite dilution,
 cm^2/sec

T is temperature, $^{\circ}\text{K}$

X is a solvent factor, given in (19), dimensionless

M is molecular weight of the solvent

μ is viscosity of the solvent, cp

V_o is molal volume of the solute, given in (19),

$\text{cm}^3/\text{g-mole}$

The Othmer-Thakar's equation is:

$$D_o = \frac{14.0 \times 10^{-5}}{M_w (1.1L_s/L_w) V_m^{0.6} \mu_s} \quad (\text{A.2.2})$$

where D_o is the diffusion coefficient at infinite dilution,
 cm^2/sec

μ_w is viscosity of water, cp

L_s is latent heat of vaporization of the solvent,
cal/g-mole

L_w is latent heat of vaporization of water, cal/g-mole

V_m is molal volume of the diffusing substance (solute),
 $\text{cm}^3/\text{g-mole}$

μ_s^0 is viscosity of the solvent at 20°C , cp

Following is a summary of calculations for diffusivities at infinite dilution of the four non-electrolyte systems covered in this project.

Diffusion coefficients at infinite dilution ($10^{-5} \text{ cm}^2/\text{sec}$)			
System*	Wilke & Chang	Othmer & Thakar	This work (extrapolated)
Sucrose-Water	0.53	0.49	0.44
Glycine-Water	1.21	1.12	0.95
Ethyl Acetate-Water	1.04	0.97	0.75
Benzene- CCl_4	1.54	0.90	1.21

Table A.1 Estimation of Diffusivities at Infinite Dilution

*In these calculations, the diffusion of the first substance to the second was considered.

System*	T (°K)	X	M	μ (Cp)	V_O or V_m (cm ³ /g-mole)	μ_w (Cp)	L_S L_w (Cal/g-mole)	μ_S^O (Cp)	
Sucrose-Water	298.16	2.6	18.02	0.894	340.4	0.894	560.0	560.0	1.000
Glycine-Water	298.16	2.6	18.02	0.894	82.6	0.894	560.0	560.0	1.000
Ethyl Acetate-Water	298.16	2.6	18.02	0.894	103.6	0.894	560.0	560.0	1.000
Benzene-CCl ₄	298.16	0.7	153.84	0.955	96.0	0.894	560.0	49.0	1.020

Table A.1 (continued) Estimation of Diffusivities at Infinite Dilution

*In these calculations, the diffusion of the first substance to the second was considered.

Since NaCl is an electrolyte, the diffusion coefficient of the NaCl-H₂O system was estimated according to Nernst's equation (21).

$$D_0 = 8.931 \times 10^{-10} T \frac{l_+^0 l_-^0}{\Lambda^0} \left(\frac{z_+ + z_-}{z_+ z_-} \right) \quad (\text{A.2.3})$$

where D_0 is the diffusivity of molecule at infinite dilution,
cm²/sec

T is absolute temperature, °K

l_+^0 is cationic conductance at infinite dilution,
mhos/equivalent

l_-^0 is anionic conductance at infinite dilution,
mhos/equivalent

$\Lambda^0 = l_+^0 + l_-^0$ is electrolyte conductance at infinite
dilution, mhos/equivalent

T is absolute temperature, °K

z_+ is valence of cation

z_- is valence of anion

According to Robinson and Stokes⁽⁵⁶⁾, we have at 25°C, for NaCl diffusing in water:

$$l_+^0 = 50.1$$

$$l_-^0 = 76.35$$

On the other hand,

$$z_+ = z_- = 1$$

Thus, the diffusivity of the NaCl-H₂O system at 25°C and infinite dilution is:

$$D_0 = 8.931 \times 10^{-10} \times 298.16 \frac{(50.1 \times 76.35)}{50.1 \times 76.35} \frac{(1 + 1)}{1 \times 1}$$

$$\underline{D_o} = 1.61 \times 10^{-5} \text{ cm}^2/\text{sec}$$

compared with the value of $\underline{1.08 \times 10^{-5} \text{ cm}^2/\text{sec}}$ found by extrapolation of the diffusion coefficient-concentration curve obtained in this project for the $\text{NaCl-H}_2\text{O}$ system at 25°C .

Appendix IIIComputer Programs

- Program A - Calculation of diffusion coefficients from moiré curves.
- Program B - Calculations of standard deviations, percent standard deviations of diffusion coefficients at different concentrations. Fitting the values of diffusion coefficient vs concentration into polynomials by the least square method to find the best fitted polynomial.
- Program C - Determination of the concentration profile from the expression $D = D(C)$ found for each system, using MIMIC.

PROGRAM A

PROGRAM TO CALCULATE DIFFUSION COEFFICIENTS FROM MOIRE CURVE

NSYST.....IS NUMBER OF SYSTEMS TO CALCULATE DIFFUSIVITIES
NPROB.....IS NUMBER OF RUNS IN EACH SYSTEM
TIT.....IS NAME OF SYSTEM
DA.....IS DENSITY OF SOLUTE
DB.....IS DENSITY OF SOLVENT
AM.....IS MOLECULAR WEIGHT OF SOLUTE
BM.....IS MOLECULAR WEIGHT OF SOLVENT
XX.....IS DISTANCE IN THE X-DIRECTION ON MAGNIFIED PICTURE ,
CM
YY.....IS HEIGHT OF MAGNIFIED MOIRE CURVE , CM
XXC.....IS DISTANCE FROM BOUNDARY , CM
YYC.....IS CORRECT HEIGHT OF MOIRE CURVE , CM
CONC.....IS CONCENTRATION OF THE DIFFUSING SPECIES CONSIDERED,
GMOLE/L
CO1.....IS INITIAL CONCENTRATION , GMOLE/L
T.....IS DIFFUSION TIME , SEC
XM.....IS MAGNIFICATION FACTOR
N.....IS THE NUMBER OF DATA POINTS. THE FIRST ONE IS XX=0.0
LIMIT.....IS THE MAXIMUM NUMBER OF SEARCHES
BMANN.....IS BOLTZMANN VARIABLE , CM/SEC**0.5
F.....IS THE FIBONACCI NUMBER

DIMENSION TIT(9),XX(60),YY(60),CONC(60),CO(60),AREA(60),DC(60),
1DERIV(60),ACX(60),AXX(60),F(25),XXM(60),COO(60),DCC(60),CONCEN(60)
1,DIFFCO(60),XXC(60),YYC(60),BMANN(60),FRMOLE(60)
COMMON XX, CONC, N, CO1
READ(5,3000)NSYST
DO 7777 ISYST=1,NSYST
READ(5,2999)TIT
WRITE(6,2001)TIT
READ(5,2998)DA,DB,AM,BM
WRITE(6,2000)DA,DB,AM,BM
READ(5,2997)NPROB
NNN=0
777 READ (5,2996) CO1, T, XM, N, LIMIT
WRITE(6,1999)CO1,T,XM,N,LIMIT
WRITE(7,1999)CO1,T,XM,N,LIMIT
NN1 = N-1
NN2=N-2
AREA(1) = 0.0
READ (5,2995) (XX(I), YY(I), I = 1,N)
DO 301 I = 2,N
XX(I)=XX(I)*0.9763
AREA(I) = ((YY(I)+YY(I-1))/2.0)*(XX(I)-XX(I-1)) + AREA(I-1)
301 CONTINUE
DO 302 I = 1,N
CONC(I) = AREA(I)/AREA(N)

```

      CO(I) = CO1 * CONC(I)
302 CONTINUE
C
C
C FIBONACCI SEARCH FOR LOCATING THE NEW ZERO POINT ON THE DIFFERENTIAL
C DEFINE FIBONACCI SERIES UP TO F(25)
      F(1)=1.0
      F(2)=2.0
      DO 7 LLL=3,25
        7 F(LLL)=F(LLL-1)+F(LLL-2)
C LIMIT DEFINES ACCURACY BY SPECIFYING NUMBER OF TIMES FIBONACCI
C SEARCH IS CARRIED OUT
C DEFINE SEARCH RANGE
      X0 = XX(1)
      XN = XX(N)
      Y0=DARINT(X0)
      YN=DARINT(XN)
C PLACEMENT OF FIRST CALCULATION
C THIS ASSUMES THAT EPSILON/F(LIMIT) IS NEGLIGIBLE
      S=(XN-X0)*(F(LIMIT-1)/F(LIMIT))
      X1=XN-S
      X2=X0+S
      Y1=DARINT(X1)
      Y2=DARINT(X2)
C FIBONACCI SEARCH FOR MINIMUM OF DARINT
C INTERIOR CALCULATIONS ARE PLACED SYMMETRICALLY
      LL=LIMIT-2
      DO 8 NOFIB=1,LL
        IF(Y1.GE.Y2) GO TO 9
        XN=X2
        YN=Y2
        X2=X1
        Y2=Y1
        X0=X0
        Y0=Y0
        X1=X0+(XN-X2)
        Y1=DARINT(X1)
        IF(X1.LT.X2) GO TO 8
        XXX = X1
        YYY = Y1
        X1=X2
        Y1=Y2
        X2 = XXX
        Y2 = YYY
        GO TO 8
9      X0=X1
        Y0=Y1
        X1=X2
        Y1=Y2
        XN=XN
        YN=YN
        X2=XN-(X1-X0)
        Y2=DARINT(X2)
        IF(X1.LT.X2) GO TO 8
        XXX = X1
        YYY = Y1
        X1=X2
        Y1=Y2

```

```

      X2 = XXX
      Y2 = YYY
      8 CONTINUE
C R IS THE MIDPOINT OF THE FINAL INTERVAL
      R=(X1+X2)/2.0
      DO 1113 I=1,N
      XXC(I)=(R-XX(I))/XM
      BMANN(I)=XXC(I)/SQRT(T)
      YYC(I)=YY(I)/XM
1113 CONTINUE
      WRITE(6,1998)
      WRITE(7,1998)
      WRITE(6,1997)(YY(I),XX(I),CO(I),XXC(I),YYC(I),BMANN(I),I=1,N)
      WRITE(7,1997)(YY(I),XX(I),CO(I),XXC(I),YYC(I),BMANN(I),I=1,N)
      WRITE(6,1996)R
C
C
C THE FOLLOWING SECTION CALCULATES THE INTEGRAL UNDER THE CURVE
C OF CONCENTRATION VERSUS DISTANCE FOR VARIOUS DISTANCES.
C
C AREA1 IS THE TOTAL AREA UNDER THE CURVE UP TO R.
C AREA2 IS THE AREA ABOVE THE CURVE MINUS AREA1.
C ACX IS A DIFFERENTIAL AREA.
C AXX IS THE TOTAL AREA UNDER THE CURVE UP TO XX.
C
C
      ACX(1) = 0.0
      AXX(1) = 0.0
      AREA1 = 0.0
      AREA2 = 0.0
      DO 77 I = 1,NN1
      IF (XX(I+1).GT.R) GO TO 78
      ACX(I+1) = (CONC(I+1)-CONC(I))*(XX(I+1)-XX(I))/2.0
      RECT = (CONC(I+1)-CONC(I))*(R-XX(I+1))
      AXX(I+1) = ACX(I+1) + RECT + AXX(I)
      AREA1 = AXX(I+1)
      GO TO 77
78   ACX(I+1) = (CONC(I+1)-CONC(I))*0.5*(XX(I+1)+XX(I)-2.0*R)
      AREA2 = ACX(I+1) + AREA2
      AXX(I+1) = AREA1 - AREA2
77 CONTINUE
C
C
C THIS SECTION CALCULATES THE DIFFUSION COEFFICIENT.
C
C DERIV IS THE DERIVATIVE OF THE CURVE.
C DC IS THE DIFFUSION COEFFICIENT IN CM. SQUARED PER SECOND.
C
C
      DO 82 I=3,NN2
      DERIV(I) = (-CONC(I+2)+8.0*CONC(I+1)-8.0*CONC(I-1)+CONC(I-2))/(12.
10*(XX(I+1)-XX(I)))
      DC(I) = AXX(I)/(2.0*T*DERIV(I)*XM*XM)
82 CONTINUE
C
C
C INTERPOLATION TO GET DIFFUSION COEFFICIENTS AT FIXED INTERVALS OF
C CONCENTRATION

```

```

C
DO 1110 I=3,NN2
  NJ=I-2
  COO(NJ)=CO(I)
1110 DCC(NJ)=DC(I)
  NN=N-4
  I1=1
  DO 1111 JK=1,9
    CONCEN(JK)=CO1/10.0*FLOAT(JK)
    FRMOLE(JK)=CONCEN(JK)/(CONCEN(JK)+(1000.0-CONCEN(JK)*AM/DA)*DB/BM)
    DO 1112 II=I1,NN
      IF(CONCEN(JK).GT.COO(II))GO TO 1112
      DIFFCO(JK)=DCC(II-1)+(DCC(II)-DCC(II-1))/(COO(II)-COO(II-1))*(CONC
1EN(JK)-COO(II-1))
      I1=II+1
      GO TO 1111
1112 CONTINUE
1111 CONTINUE
  WRITE(6,1995)
  WRITE(7,1995)
  WRITE(6,1994)(CONCEN(JI),FRMOLE(JI),DIFFCO(JI),JI=1,9)
  WRITE(7,1994)(CONCEN(JI),FRMOLE(JI),DIFFCO(JI),JI=1,9)

```

```

C
C
  NNN = NNN+1
  IF(NNN.LT.NOPROB) GO TO 777
7777 CONTINUE
3000 FORMAT(I3)
2999 FORMAT(9A5)
2998 FORMAT(2F6.3,2F6.2)
2997 FORMAT(I5)
2996 FORMAT(3F10.3,2I5)
2995 FORMAT(2F10.2)
2001 FORMAT(1H1,9A5////)
2000 FORMAT(5X,19HDENSITY OF SOLUTE =,F6.3,3X,20HDENSITY OF SOLVENT =,
1F6.3//5X,18HMOL WT OF SOLUTE =,F7.2,3X,19HMOL WT OF SOLVENT =,F7.2
1)
1999 FORMAT(1H1,5X,5HCO1 =,F6.3,4H N ,3HT =,F9.2,6H SEC ,4HXM =,F6.2,
15H N =,I3,2X,7HLIMIT =,I3//)
1998 FORMAT(8X,2HYY,8X,2HXX,7X,2HCO,5X,7HCOR. XX,3X,7HCOR. YY,3X,18HBOL
1TZMANN VARIABLE/7X,4H(CM),6X,4H(CM),3X,9H(GMOLE/L),3X,4H(CM),6X,4H
1(CM),5X,13H(CM/SEC**0.5)/)
1997 FORMAT(1H ,5F10.3,6X,E10.3)
1996 FORMAT(1H0,4HR IS,F8.4)
1995 FORMAT(1H1,5X,13HCONCENTRATION,3X,13HMOLE FRACTION,3X,21HDIFFUSION
1 COEFFICIENT/8X,9H(GMOLE/L),25X,11H(CM**2/SEC)/)
1994 FORMAT(5X,F10.3,7X,F10.3,10X,E10.3)
  STOP
  END

```

```

C
C
C
$IBFTC DARINT
  FUNCTION DARINT(RR)
C FUNCTION SUBPROGRAM FOR CALCULATING THE DIFFERENCE BETWEEN THE AREAS,
C DARINT, ON EACH SIDE OF THE SELECTED ZERO POINT USING TRAPEZOIDAL RULE
  DIMENSION TIT(9),XX(60),YY(60),CONC(60),CO(60),AREA(60),DC(60),
1DERIV(60),ACX(60),AXX(60),F(25),XXM(60),COO(60),DCC(60),CONCEN(60)

```

```

1,DIFFCO(60),XXC(60),YYC(60),BMANN(60),FRMOLE(60)
COMMON XX, CONC, N, CO1
C LOCATION OF RR IN PROPER INTERVAL ON XX(I) AXIS
DO 1 I=1,N
IF(XX(I).GT.RR)GO TO 2
1 CONTINUE
2 I=I-1
C CALCULATION OF SUBAREA BETWEEN XX(I) AND RR
C HR IS CURVE HEIGHT AT RR
HR=CONC(I)+(RR-XX(I))*(CONC(I+1)-CONC(I))/(XX(I+1)-XX(I))
C CALCULATION OF AVERAGE HEIGHT, HAVG1, IN SUBINTERVAL AND SUBAREA,
C SUBA1
HAVG1 = (HR + CONC(I))/2.0
SUBA1 = HAVG1*(RR-XX(I))
SAREA=0.0
CAREA = 0.0
C CALCULATION OF AREA UNDER CURVE UP TO XX(I) AND AREA UP TO RR,ARINT1
NN=I-1
IF(NN .EQ. 0) GO TO 4200
DO 3 J=1,NN
CAREA = (XX(J+1) - XX(J))*(CONC(J+1) + CONC(J))/2.0
3 SAREA = SAREA + CAREA
GO TO 4201
4200 CAREA = 0.0
SAREA = 0.0
4201 ARINT1=SAREA+SUBA1
C CALCULATION OF SUBAREA BETWEEN RRAND XX(I+1), SUBA2
C CONC(I) IS REPLACED BY (CO1-CONC(I+1))
HR = CONC(N) - HR
HAVG2= (HR+CONC(N)-CONC(I+1))/2.0
SUBA2 = HAVG2*(XX(I+1)-RR)
CAREA = 0.0
SAREA=0.0
C CALCULATION OF AREA UNDER CURVE FROM RR TO XX(N)
IJ=I+1
NN=N-1
DO 4 J=IJ,NN
CAREA = (XX(J+1)-XX(J))*(2.0*CONC(N)-CONC(J+1)-CONC(J))/2.0
4 SAREA = SAREA + CAREA
ARINT2=SAREA+SUBA2
DARINT=ABS(ARINT2-ARINT1)
RETURN
END

```

```

-----
PROGRAM B
-----

```

CALCULATIONS OF MEAN DIFFUSION COEFFICIENTS, STANDARD DEVIATIONS
AND PERCENT OF STANDARD DEVIATIONS

MDC.....IS MEAN DIFFUSION COEFFICIENT
SQDEV.....IS SQUARE OF DEVIATION
STDDEV.....IS STANDARD DEVIATION
PCSTDV.....IS PERCENT OF STANDARD DEVIATION
PCSTDV.....IS PERCENT STANDARD DEVIATION (MEAN/STD DEV)
DCPOLY.....IS VALUE OF DIFFUSION COEFFICIENT AFTER FITTING
DEVNEW.....IS STANDARD OF DEVIATION AFTER FITTING
PCDNEW.....IS PERCENT STANDARD DEVIATION AFTER FITTING
ASUMPC.....IS THE AVERAGE OF PERCENT STD DEV

```

DOUBLE PRECISION CO(10,10),DC(10,10),MDC(10),SQDEV(10),STDDEV(10),
1PCSTDV(10),A(9),COO(100),DCC(100),AA(100),POLY(8),DCPOLY(8),SUMSQ(
110),DEVNEW(10),PCDNEW(10),FRMOLE(10,10)

```

```

REAL MDC

```

```

READ(5,998)NPROB

```

```

DO 1000 II=1,NPROB

```

```

READ(5,996)A

```

```

WRITE(6,999)A

```

```

WRITE(7,999)A

```

```

READ(5,994)((CO(I,J),FRMOLE(I,J),DC(I,J),I=1,9),J=1,8)

```

```

SUMPC=0.0

```

```

DO 2000 I=1,9

```

```

MDC(I)=0.0

```

```

DO 3000 J=1,8

```

```

MDC(I)=MDC(I)+DC(I,J)

```

```

3000 CONTINUE

```

```

MDC(I)=MDC(I)/8.0

```

```

SQDEV(I)=0.0

```

```

DO 4000 J=1,8

```

```

SQDEV(I)=SQDEV(I)+(DC(I,J)-MDC(I))**2

```

```

4000 CONTINUE

```

```

STDDEV(I)=SQRT(SQDEV(I)/8.0)

```

```

PCSTDV(I)=STDDEV(I)/MDC(I)*100.0

```

```

SUMPC=SUMPC+PCSTDV(I)

```

```

2000 CONTINUE

```

```

ASUMPC=SUMPC/9.0

```

```

WRITE(6,997)

```

```

WRITE(7,997)

```

```

WRITE(6,995)(CO(I,1),MDC(I),STDDEV(I),PCSTDV(I),I=1,9)

```

```

WRITE(7,995)(CO(I,1),MDC(I);STDDEV(I),PCSTDV(I),I=1,9)

```

```

WRITE(6,989)ASUMPC

```

```

WRITE(7,989)ASUMPC

```

```

C   FITTING DIFFUSION COEFFICIENTS VS CONCENTRATION TO A POLYNOMIAL
C   BY THE LEAST SQUARE METHOD
C
      I1=1
      DO 5100 I=1,9
      DO 5200 J=1,8
      COO(I1)=CO(I,J)
      DCC(I1)=DC(I,J)
      I1=I1+1
5200 CONTINUE
5100 CONTINUE
      N=72
      M=1
      DO 5600 M1=1,8
      POLY(M1)=0.0
5600 CONTINUE
5000 CALL DLESQ(AA,POLY,COO,DCC,M,N)
      M1=M+1
      WRITE(6,987)
      WRITE(6,993)POLY
      WRITE(7,993)POLY
      SUMPC=0.0
      DO 5300 I=1,9
      DCPOLY(I)=POLY(1)
      DO 5400 JK=2,M1
      DCPOLY(I)=DCPOLY(I)+POLY(JK)*CO(I,1)**(JK-1)
5400 CONTINUE
      SUMSQ(I)=0.0
      DO 5500 J=1,8
      SUMSQ(I)=SUMSQ(I)+(DC(I,J)-DCPOLY(I))**2
5500 CONTINUE
      DEVNEW(I)=SQRT(SUMSQ(I)/8.0)
      PCDNEW(I)=DEVNEW(I)/DCPOLY(I)*100.0
      SUMPC=SUMPC+PCDNEW(I)
5300 CONTINUE
      ASUMPC=SUMPC/9.0
      WRITE(6,991)
      WRITE(7,991)
      WRITE(6,995)(CO(I,1),DCPOLY(I),DEVNEW(I),PCDNEW(I),I=1,9)
      WRITE(7,995)(CO(I,1),DCPOLY(I),DEVNEW(I),PCDNEW(I),I=1,9)
      WRITE(6,989)ASUMPC
      WRITE(7,989)ASUMPC
      M=M1
      IF(M.LT.8)GO TO 5000
1000 CONTINUE
      998 FORMAT(I5)
      996 FORMAT(9A6)
      994 FORMAT(5X,F10.3,7X,F10.3,10X,E10.3)
      999 FORMAT(1H1,5X,9A6///)
      997 FORMAT(6X,5HCONC.,4X,14HMEAN DIFF. CO.,4X,18HSTANDARD DEVIATION,4X
      1,17HPERCENT STD. DEV./)
      995 FORMAT(1H ,F10.3,5X,E10.3,12X,E10.3,7X,F10.3)
      993 FORMAT( 10X,E12.5,10X,E12.5)
      991 FORMAT( ///6X,5HCONC.,4X,14HBEST FITTED DC,4X,18HSTANDARD DEVIATIO
      1N,4X,17HPERCENT STD. DEV./)
      989 FORMAT( /10X,27HAVERAGE PERCENT STD. DEV. =,F7.2)
      987 FORMAT( /////15X,23HPOLYNOMIAL COEFFICIENTS/)
      STOP

```



```

09T1      EQL((C10-C08)*(C10-C08)/4.0)
09T2      EQL(C10-2.0*C09+C08)
09F       EQL(A0+(A1+(A2+(A3+(A4+A5*C09)*C09)*C09)*C09)*C09)
09G       EQL(A1+(A2+(A3+(A4+A5*C09)*C09)*C09)*C09)
C09       INT(K*(09T1*09G+09T2*09F),CAVER)
10T1      EQL((C11-C09)*(C11-C09)/4.0)
10T2      EQL(C11-2.0*C10+C09)
10F       EQL(A0+(A1+(A2+(A3+(A4+A5*C10)*C10)*C10)*C10)*C10)
10G       EQL(A1+(A2+(A3+(A4+A5*C10)*C10)*C10)*C10)
C10       INT(K*(10T1*10G+10T2*10F),C17)
11T1      EQL((C12-C10)*(C12-C10)/4.0)
11T2      EQL(C12-2.0*C11+C10)
11F       EQL(A0+(A1+(A2+(A3+(A4+A5*C11)*C11)*C11)*C11)*C11)
11G       EQL(A1+(A2+(A3+(A4+A5*C11)*C11)*C11)*C11)
C11       INT(K*(11T1*11G+11T2*11F),C17)
12T1      EQL((C13-C11)*(C13-C11)/4.0)
12T2      EQL(C13-2.0*C12+C11)
12F       EQL(A0+(A1+(A2+(A3+(A4+A5*C12)*C12)*C12)*C12)*C12)
12G       EQL(A1+(A2+(A3+(A4+A5*C12)*C12)*C12)*C12)
C12       INT(K*(12T1*12G+12T2*12F),C17)
13T1      EQL((C14-C12)*(C14-C12)/4.0)
13T2      EQL(C14-2.0*C13+C12)
13F       EQL(A0+(A1+(A2+(A3+(A4+A5*C13)*C13)*C13)*C13)*C13)
13G       EQL(A1+(A2+(A3+(A4+A5*C13)*C13)*C13)*C13)
C13       INT(K*(13T1*13G+13T2*13F),C17)
14T1      EQL((C15-C13)*(C15-C13)/4.0)
14T2      EQL(C15-2.0*C14+C13)
14F       EQL(A0+(A1+(A2+(A3+(A4+A5*C14)*C14)*C14)*C14)*C14)
14G       EQL(A1+(A2+(A3+(A4+A5*C14)*C14)*C14)*C14)
C14       INT(K*(14T1*14G+14T2*14F),C17)
15T1      EQL((C16-C14)*(C16-C14)/4.0)
15T2      EQL(C16-2.0*C15+C14)
15F       EQL(A0+(A1+(A2+(A3+(A4+A5*C15)*C15)*C15)*C15)*C15)
15G       EQL(A1+(A2+(A3+(A4+A5*C15)*C15)*C15)*C15)
C15       INT(K*(15T1*15G+15T2*15F),C17)
16T1      EQL((C17-C15)*(C17-C15)/4.0)
16T2      EQL(C17-2.0*C16+C15)
16F       EQL(A0+(A1+(A2+(A3+(A4+A5*C16)*C16)*C16)*C16)*C16)
16G       EQL(A1+(A2+(A3+(A4+A5*C16)*C16)*C16)*C16)
C16       INT(K*(16T1*16G+16T2*16F),C17)
          HDR(T,C07,C08,C09,C10,C11)
          HDR
          OUT(T,C07,C08,C09,C10,C11)
          FIN(T,3800.0)
          END

```

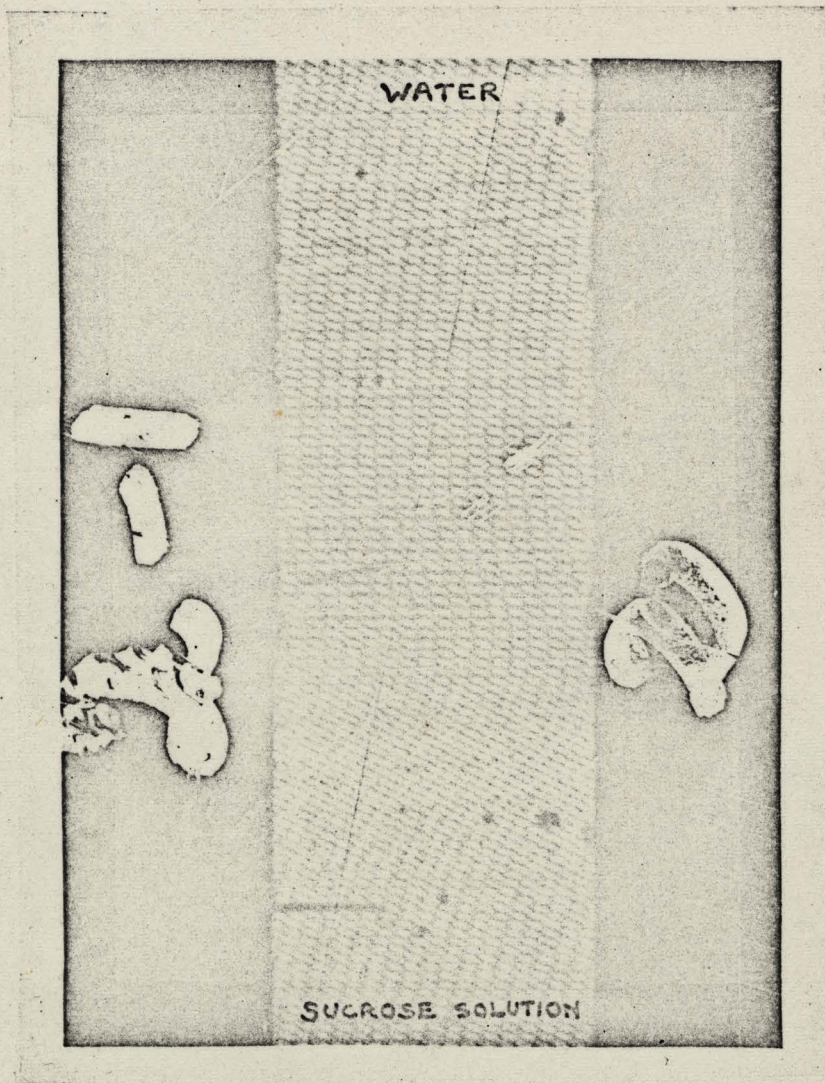


Figure 27

Sample Picture - Sucrose-Water System @ 25°C after 244 minutes of Diffusion

EQUATIONS EXPERIMENTALLY FOUND FOR DIFFUSION COEFFICIENTS AS FUNCTION OF CONCENTRATION.-

General Form:

$$D = a_0 + a_1C^1 + a_2C^2 + a_3C^3 + a_4C^4 + a_5C^5$$

$$D = \text{cm}^2/\text{sec}$$

C = gmole/l, concentration of the first substance in the following table.

System	Value of Coefficients					
	a ₀	a ₁	a ₂	a ₃	a ₄	a ₅
Sucrose-Water	0.44424 x 10 ⁻⁵	0.33786 x 10 ⁻⁴	-0.37170 x 10 ⁻³	0.14273 x 10 ⁻²	-0.23642 x 10 ⁻²	0.14244 x 10 ⁻²
NaCl-Water	0.10804 x 10 ⁻⁴	0.26287 x 10 ⁻⁴	-0.77257 x 10 ⁻⁴	0.86971 x 10 ⁻⁴	-0.41758 x 10 ⁻⁴	0.72616 x 10 ⁻⁵
EtAc-Water	0.75493 x 10 ⁻⁵	0.28566 x 10 ⁻⁴	-0.18939 x 10 ⁻³	0.40335 x 10 ⁻³	-0.28200 x 10 ⁻³	0.0
Glycine-Water	0.95558 x 10 ⁻⁵	-0.82456 x 10 ⁻⁵	0.12676 x 10 ⁻⁵	0.10214 x 10 ⁻⁴	-0.78592 x 10 ⁻⁵	0.16902 x 10 ⁻⁵
C ₆ H ₆ - CCL ₄	0.12140 x 10 ⁻⁴	0.48276 x 10 ⁻⁴	-0.73211 x 10 ⁻⁶	-0.15320 x 10 ⁻⁴	0.14067 x 10 ⁻⁴	-0.34567 x 10 ⁻⁵

Table A.2